Detection of Osseous Spinal Metastasis with T1-weighted Dynamic Contrast-enhanced Perfusion MRI and PET: Assessing Agreement in Positive Biopsy

Deeptha Bejugam BS [1,2]

Kyung K. Peck PhD[2,3], Atin Saha MD[2], Elena Yllera-Contreras MD[2], Onur Yildirim MD[2], Julio Arevajo-Perez MD PhD[2], Simone Krebs MD[2], Eric Lis MD[2], Sasan Karimi MD[2], Andrei Holodny MD[2]

1. Georgetown University School of Medicine
2. Memorial Sloan Kettering Department of Radiology
3. Memorial Sloan Kettering Department of Medical Physics

Memorial Sloan Kettering Cancer Center

Introduction

- The spine is the 3rd most frequent site for cancer metastasis, accounting for about 70% of all osseous metastases
- Conventional MRI, including STIR and T1-weighted, and ^{18}F-FDG PET/CT are standard imaging modalities

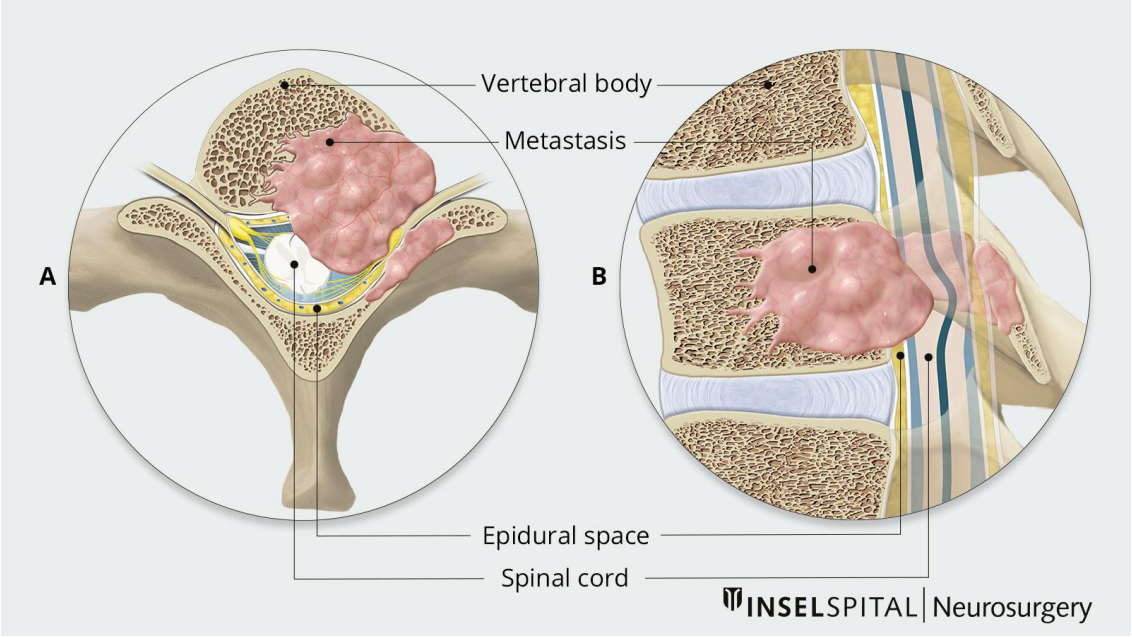

DCE-MRI

- Dynamic contrast-enhanced MRI (DCE-MRI) is an advanced imaging technique, not as routinely utilized in spine imaging

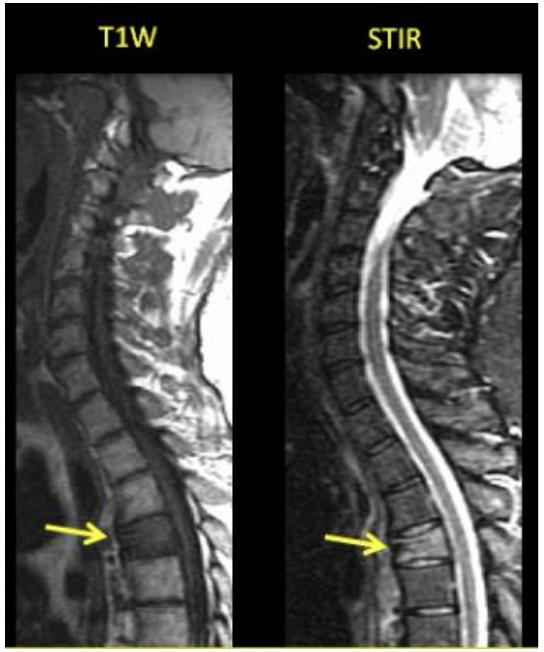

- Can differentiate between metastatic and benign vertebral lesions,[1] determine tumor characteristics,[2] and detect recurrent disease and treatment response[3]

1. Guan et al. T1-weighted Dynamic Contrast-enhanced MR imaging to Differentiate Nonneoplastic and Malignant Vertebral Body Lesions in the Spine. *Radiology*. 2020
2. Saha et al. Magnetic resonance perfusion characteristics of hypervascular renal and hypovascular prostate spinal metastases. *Spine*. 2014
3. Behar et al. T1-Weighted, Dynamic Contrast-Enhanced MR Perfusion Imaging Can Differentiate between Treatment Success and Failure in Spine Metastases Undergoing Radiation Therapy. *AJNR Am J Neuroradiol*. 2023 Dec 11

Research Gap

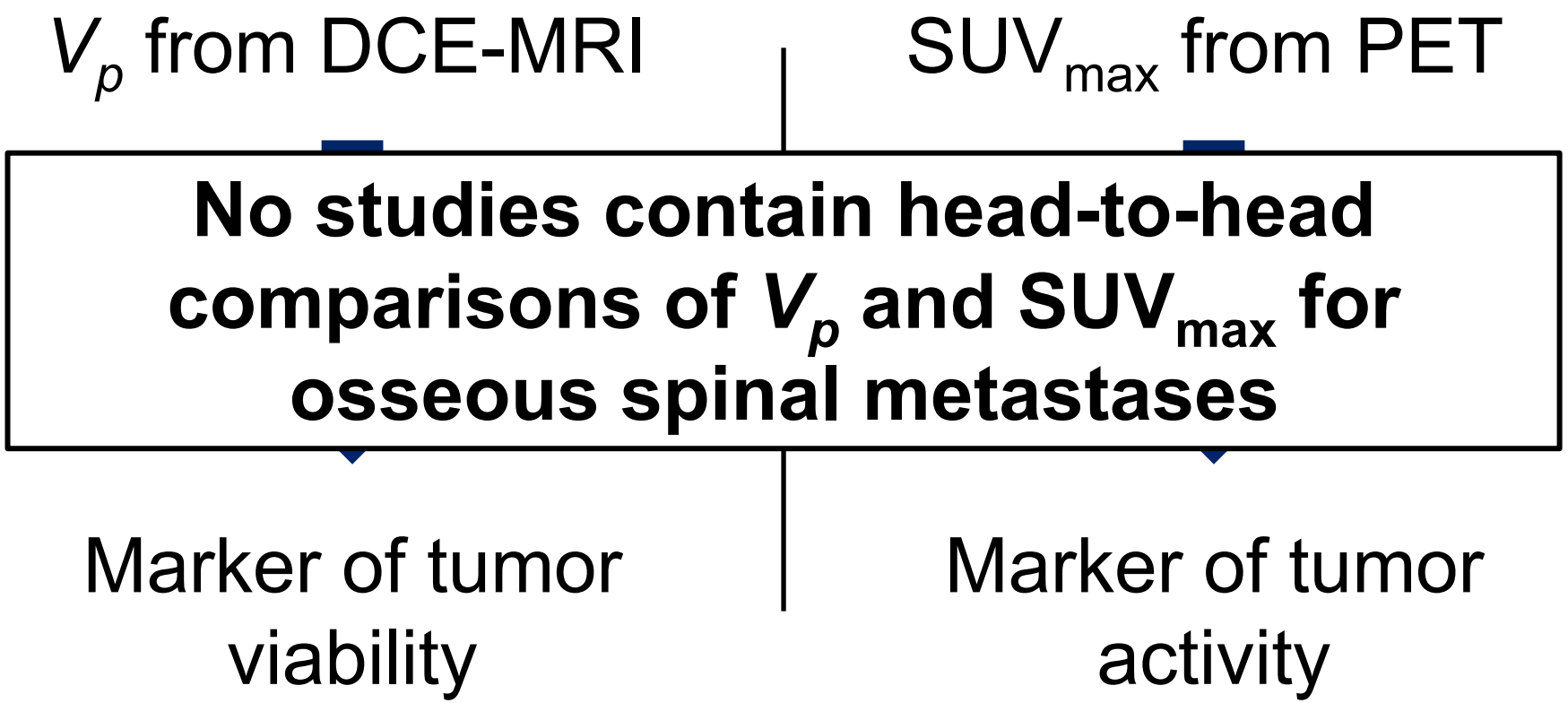

Hypothesis and Aim

Hypothesize that V_p can successfully identify biopsy-proven, non-treated osseous spinal metastases and shows high agreement with SUV_{max}

Methods: Population

Non-treated osseous spinal lesions with available DCE perfusion MRI, PET, and a correlative pathology result between February 2015 and January 2022

n=116

Excluded

n=21

- Lesions with DCE perfusion MRI and PET over 1 year apart (n=1)
- Lesions with recorded radiation therapy (RT) to a vertebrae within two vertebrae of spinal metastasis (n=6)
- Lesions with recorded non-RT treatment between DCE perfusion MRI and PET (n=14)

Non-treated osseous spinal lesions with a correlative pathology with no cancer treatment between DCE perfusion MRI and PET

n=95

Excluded

n=10

- Lesions with poor perfusion data due to noise from blood flow in the heart and aorta or patient movement during MRI (n=9)
- Lesions with lack of normal vertebrae for normalization due to prior kyphoplasty and/or surgical devices (n=1)

Lesions meeting all inclusion criteria

n=85

Population

- 85 non-treated osseous spinal metastases across 70 patients
- Common primary cancers were breast, lung, and prostate
- Average time between DCE-MRI and ^{18}F-FDG PET/CT was 1.38 days

	Count
Patients & Demographics	
No. of Patients	70
Male	36
Female	34
Mean Age (yr)	62.87
Lesion Characteristics	
No. of Lesions	85
Location	
Cervical	7
Thoracic	44
Lumbar	32
Sacral	2
Metastatic Source	
Breast	19
Lung	16
Prostate	9
Multiple Myeloma	8
Thyroid	8
Esophagus	4
Lymphoma	4
Hepatocellular Carcinoma	3
Head and Neck SCC	3
Uterine Leiomyosarcoma	2
Renal	2
Other	7
Time between DCE-MRI and PET	
Mean Days	1.38

Methods

DCE-MRI

- Gadavist injection
- 1.5T or 3T scanner
- NordicICE to calculate mean K_{trans} and V_p
- V_p threshold of 2.10 [1]

^{18}F-FDG PET/CT

- ^{18}F-FDG injection
- GE D690 time of flight system
- Visage to calculate SUV_{max}
- SUV_{max} thresholds of 2.00, 2.50, and 4.00 [2,3]

1. Saha et al. Magnetic resonance perfusion characteristics of hypervascular renal and hypovascular prostate spinal metastases. *Spine*. 2014
2. Mah K, Caldwell C. Biological Target Volume. In: *PET-CT in Radiotherapy Treatment Planning*. ; 2008.
3. Mettle Jr. F, Guiberteau M. Inflammation and Infection Imaging. In: *Essentials of Nuclear Medicine Imaging*. Sixth Edition. ; 2012.

Results

DCE-MRI Vessel Permeability (K_{trans})

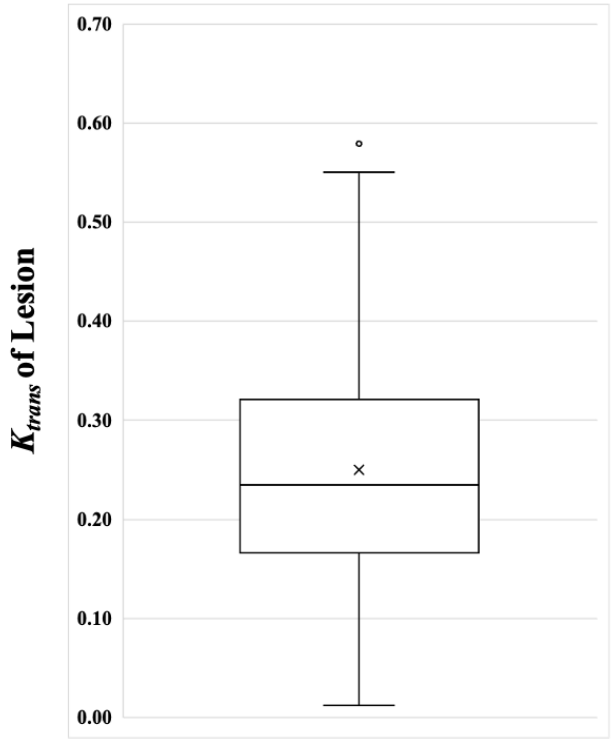

DCE-MRI Plasma Volume (V_p)

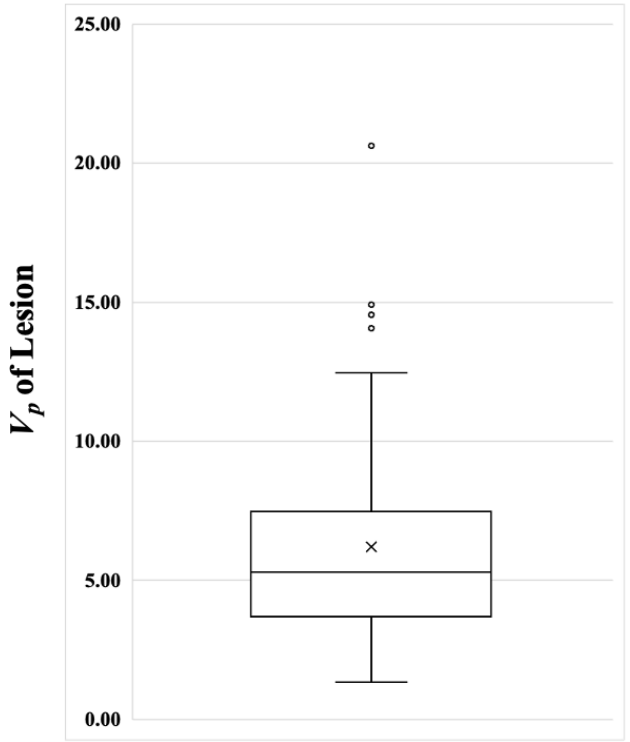

PET Standardized Uptake Value (SUV_{max})

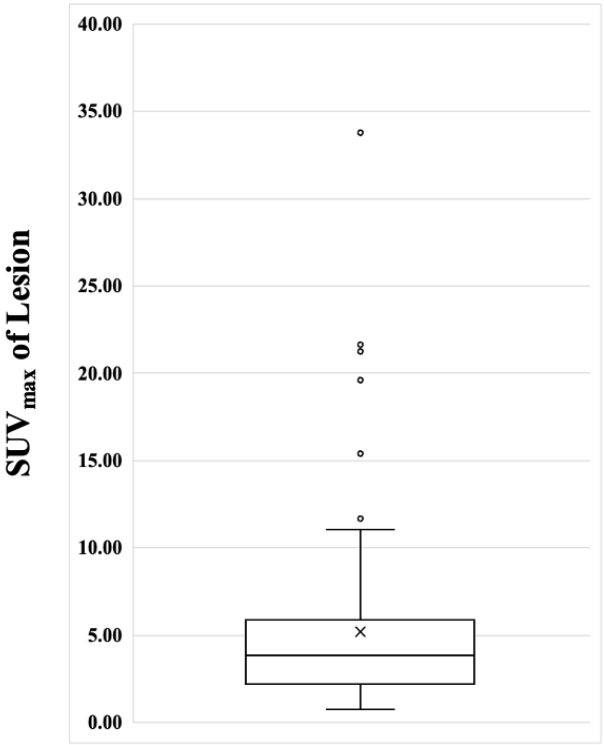

0.25 ± 0.12

6.18 ± 3.35

5.16 ± 5.23

Results

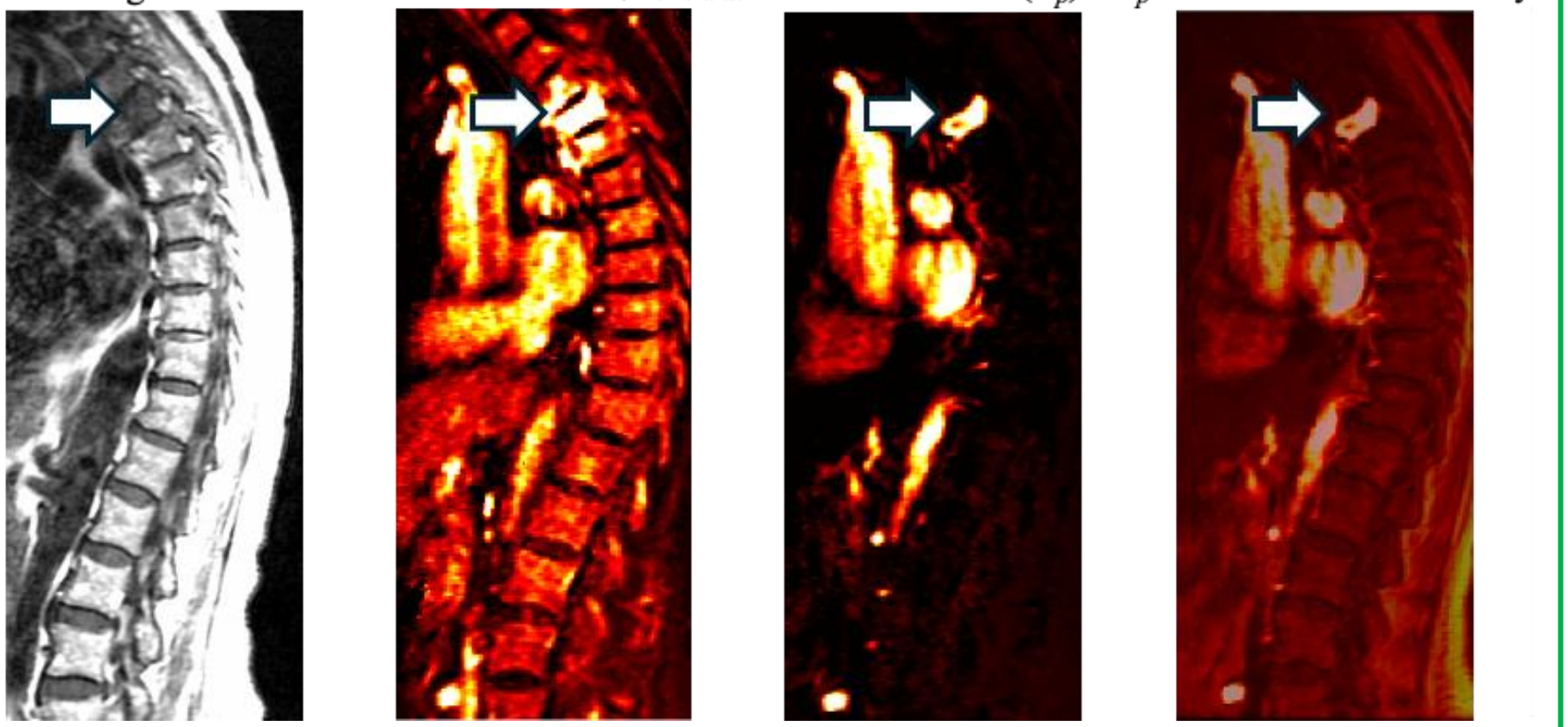

V_p of 14.05

SUV_{max} of 3.08

Results

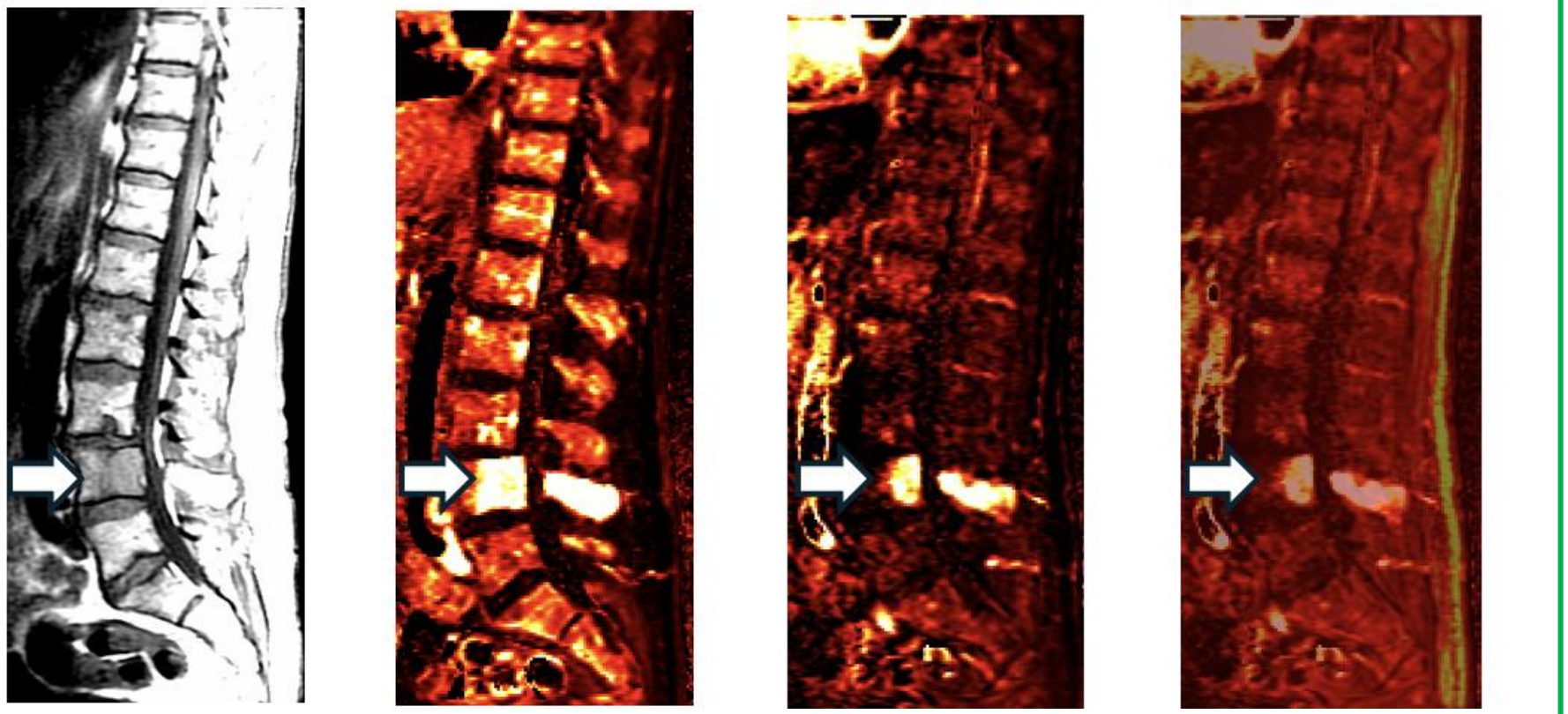

V_p of 5.77

SUV_{max} of 15.64

Results

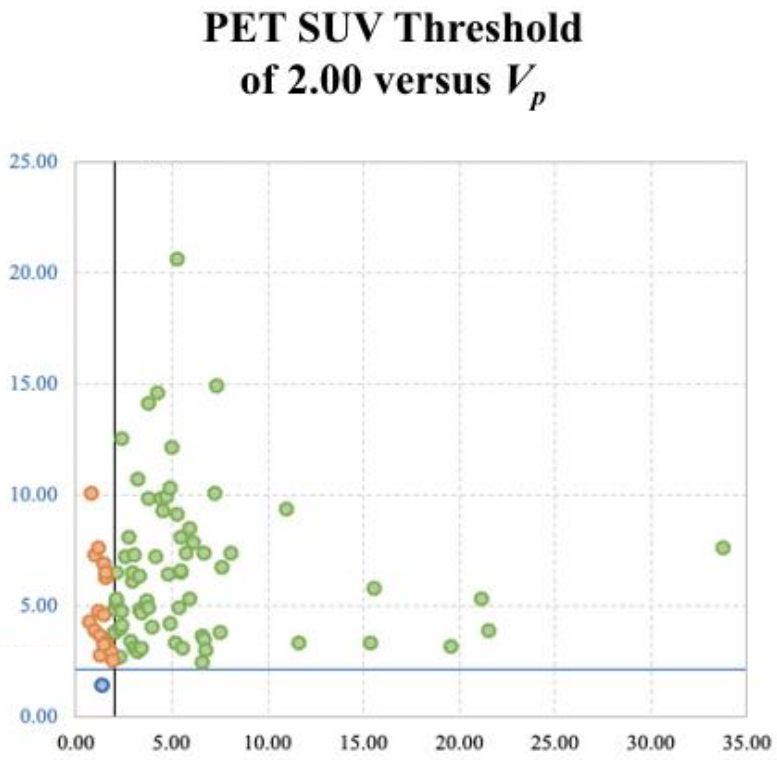

81.18%

67.06%

48.24%

Results

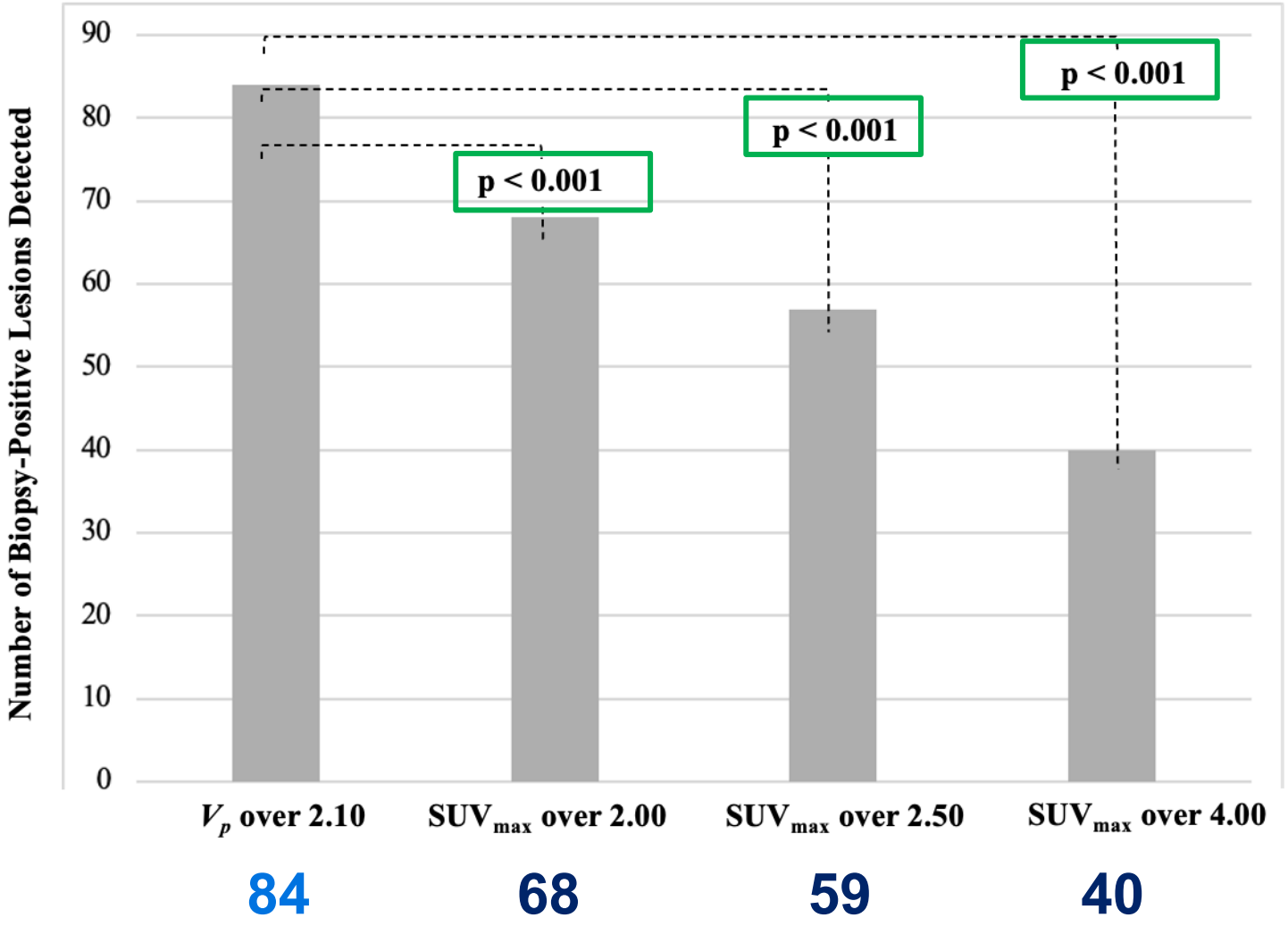
Number of Biopsy-Positive Lesions Detected
90
80
70
60
50
40
30
20
10
0
p < 0.001
p < 0.001
p < 0.001
V_p over 2.10
SUV_{max} over 2.00
SUV_{max} over 2.50
SUV_{max} over 4.00
84
68
59
40

Results

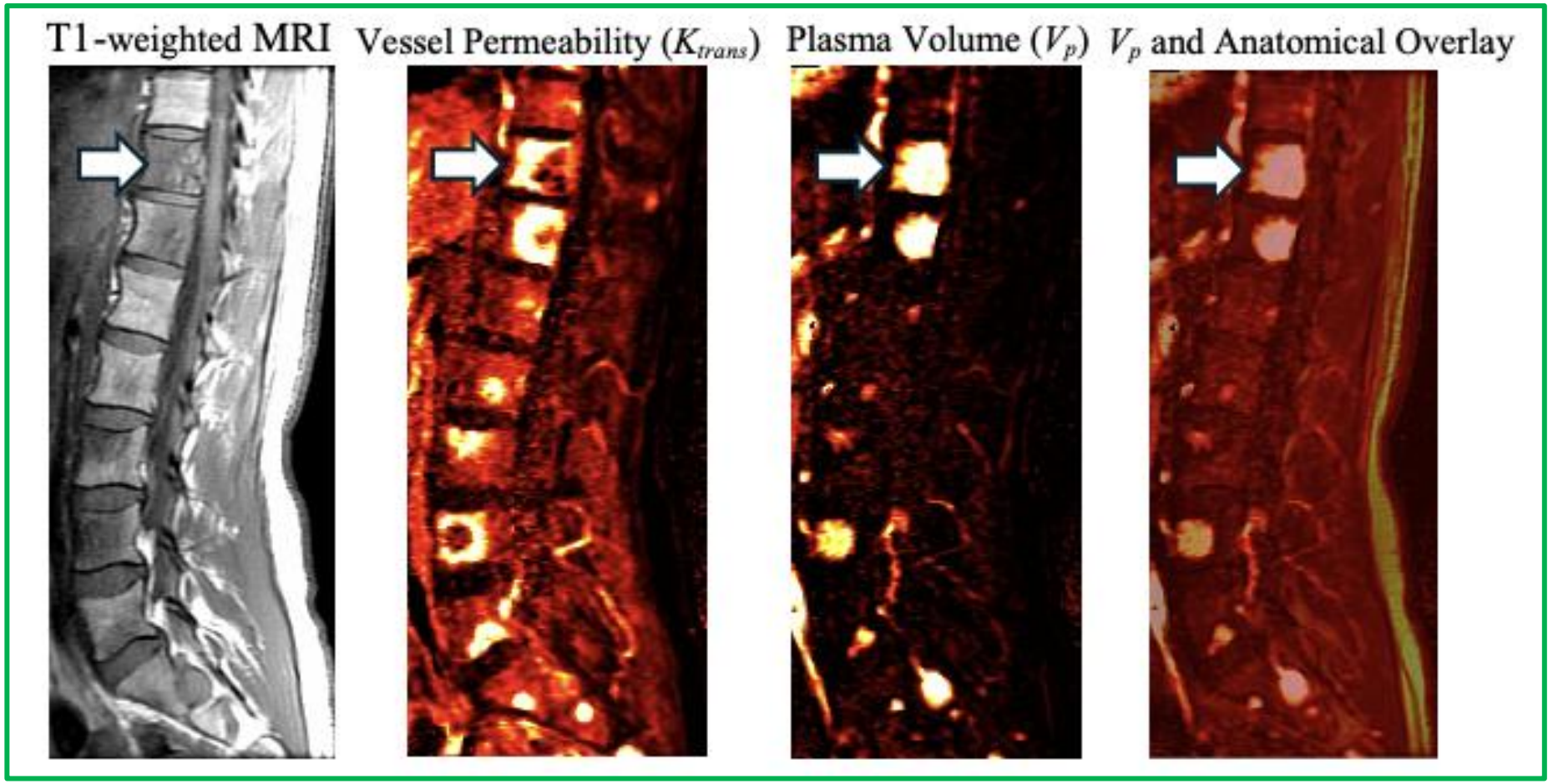

V_p of 10.01

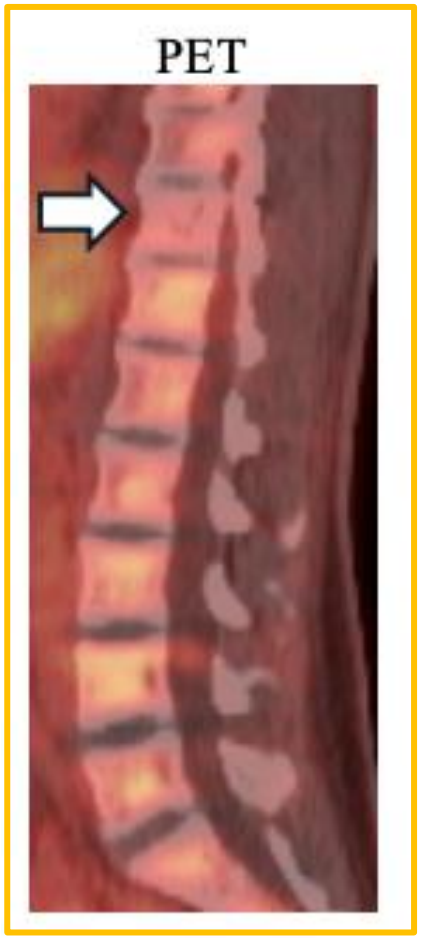

SUV_{max} of 0.86

Results

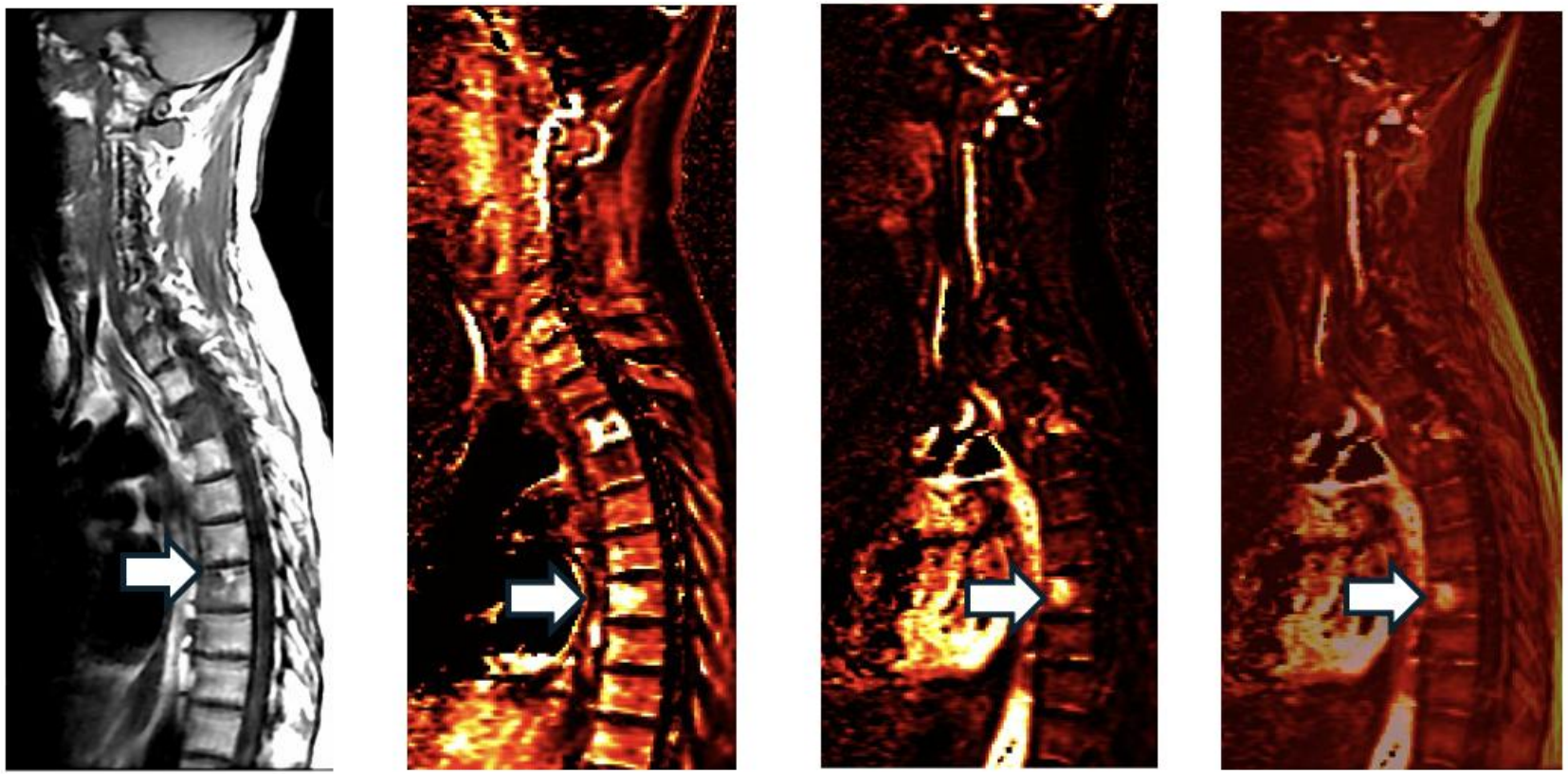

V_p of 4.21

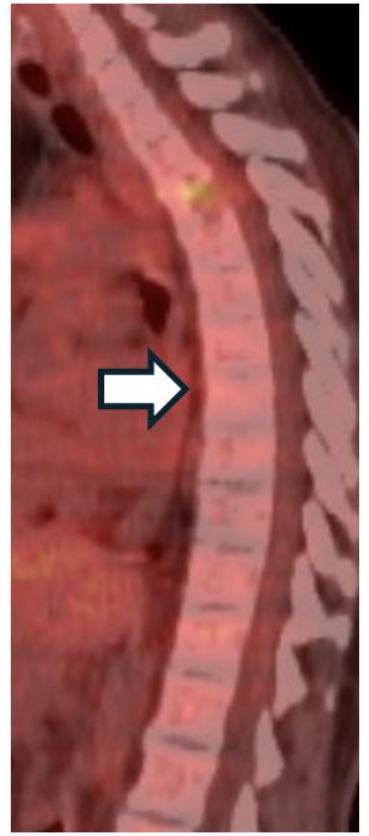

SUV_{max} of 0.72

Discussion

- At the most conservative threshold of 2.00 for SUV_{max}, V_p shows high agreement with SUV_{max} in detecting malignant tumors confirmed by biopsy.
- DCE-MRI's V_p outperforms PET SUV_{max} measurements in identifying the highest number of lesions.
- DCE-MRI’s ability to detect spinal metastases may reduce the need for radiotracer-based imaging, effectively decreasing costs and patient radiation exposure

Thank You!

Department of Radiology

Kyung K. Peck PhD
Atin Saha MD
Elena YIlera-Contreras MD
Onur Yildirim MD
Julio Arevajo-Perez MD PhD
Simone Krebs MD
Eric Lis MD
Sasan Karimi MD
Andrei Holodny MD

db1449@georgetown.edu

Memorial Sloan Kettering Cancer Center

Supplemental Methods

- MRI were performed with either 3T or 1.5 T scanner (GE Healthcare, Milwaukee, WI) by using an eight-channel cervical-thoracic-lumbar surface coil.
- All patients underwent routine clinical MRI sequences including sagittal T1 (field of view [FOV], 32–36 cm; slice thickness, 3mm; repetition time [TR], 400–650 msec; flip angle [FA], 90°), sagittal T2 (FOV, 32–36 cm; slice thickness, 3 mm; TR, 3500–4000 msec; FA, 90°), sagittal STIR ((FOV, 32–36 cm; slice thickness, 3 mm; TR, 3500–6000 msec; FA, 90).
- For DCE perfusion MRI, Gadavist® (Bayer, Barmen, Germany) was administered at 0.1 mmol/kg body weight and a rate of 2–3 mL/sec. **10 phases for pre-injection delay** were set and the contrast was administrated after the delay. Kinetic enhancement of the tissue during and after injection of the contrast was highlighted by using a three-dimensional **T1-weighted fast spoiled-gradient recalled (SPGR)** echo sequence (TR/TE, 4–5ms/1–2ms; slice thickness, 5 mm; field of view, 32 cm**; phase temporal resolution, 5~6 seconds**; and flip angle, 20°) and acquired in the sagittal plane.
- The **duration of the DCE sequence was 4-5 minutes**. Post-contrast sagittal and axial T1-weighted images were acquired after DCE perfusion MRI.

Supplemental Methods

- ^{18}F-FDG PET/CT was performed using a GE D690 time of flight system, featuring a 64-slice state-ot-the-art design with a dedicated full ring LYSO crystal PET.
- Patients fasted at least 6 hours before the exam and underwent whole-body PT/CT conventional imaging 60 minutes after injection of 390 ± 14MBq/Kg ^{18}F-FDG.
- Scans were acquired with an axial field of view from the vertex to the toes and PET/CT images were reconstructed using an ordered-subset expectation maximization algorithm and a gaussian filter using the standard manufacture-supplied reconstruction software The CT protocol was designed for attenuation correction and anatomic localization of PET abnormalities.
- For each lesion, a region of interest (ROI) was manually placed on the area of high uptake in the PET-CT scan to measure the maximum standardized uptake values (SUV_{max}), selected for its higher reproducibility.
- Standardized uptake values (SUV) were normalized to the patient's body weight and normal liver parenchyma, reflecting the highest activity concentration (SUV_{max}) at each specific disease site.

1. Park J, Chang KJ, Seo YS, et al. Tumor SUVmax Normalized to Liver Uptake on (18)F-FDG PET/CT Predicts the Pathologic Complete Response After Neoadjuvant Chemoradiotherapy in Locally Advanced Rectal Cancer. *Nucl Med Mol Imaging*. 2014;48(4):295-302. doi:10.1007/s13139-014-0289-x
2. Lee JW, Paeng JC, Kang KW, et al. Prediction of tumor recurrence by 18F-FDG PET in liver transplantation for hepatocellular carcinoma. *J Nucl Med*. 2009;50(5):682-687.

Results

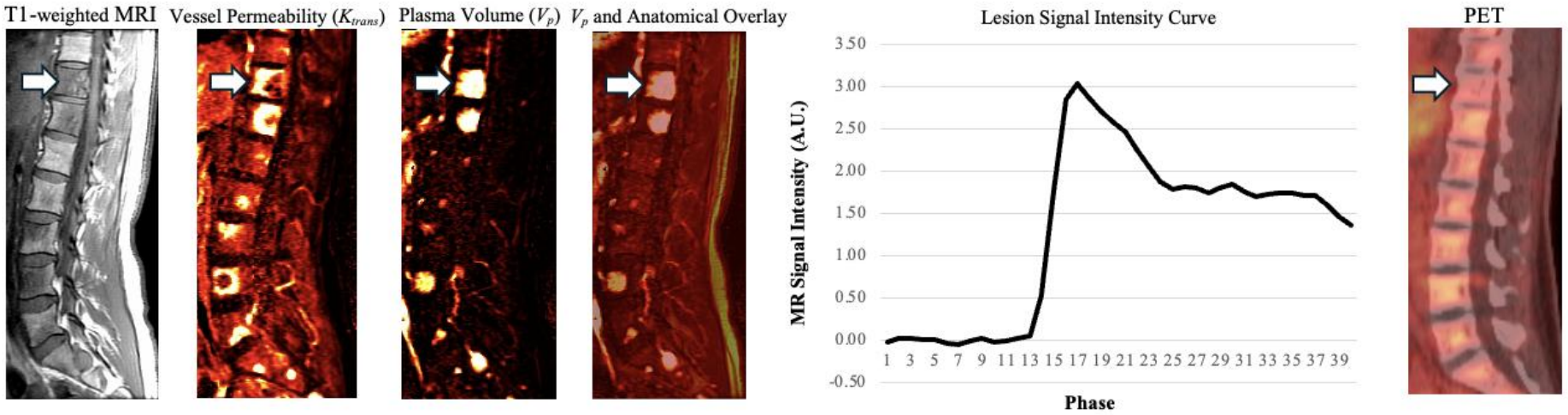

- 29 y/o M with a pathologically confirmed T11 metastasis from pulmonary carcinoid cancer.
- K_{trans} and V_p maps show high qualitative enhancement at the lesions with a K_{trans} value of 0.3520 and a *Vp* value of 10.01.
- Corresponding PET/CT is non-avid at T11 with a SUV_{max} of 0.86

Results

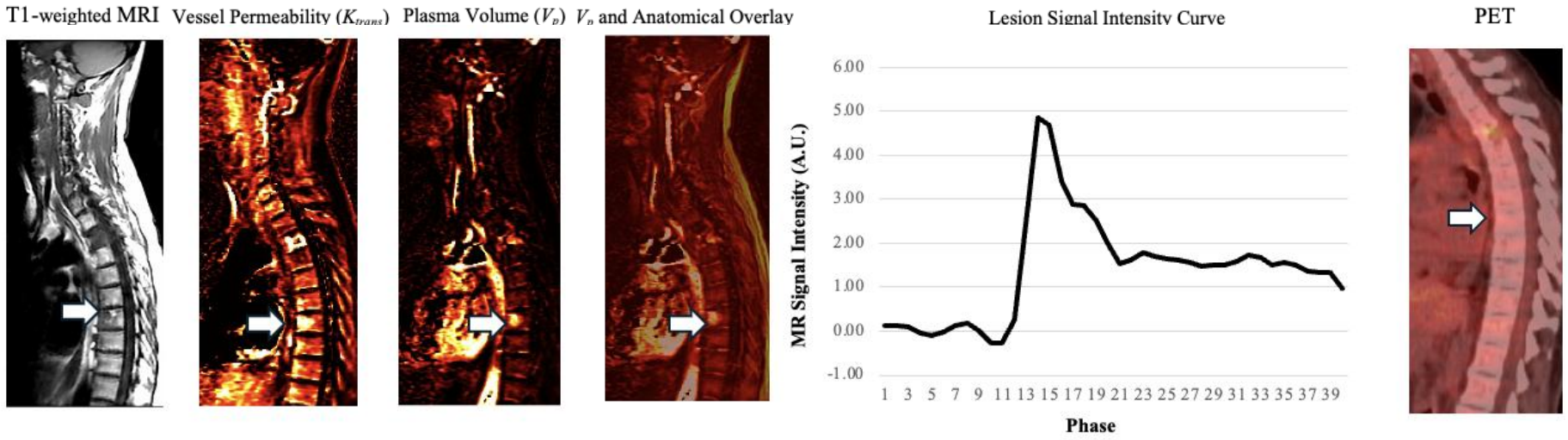

- 46 y/o F with thyroid cancer with pathologically proven metastasis to T7.
- K_{trans} map shows qualitative enhancement at the anterior aspect of T7 body with a K_{trans} of 0.2600 and V_p map shows perfusion in those regions with a noted value of 5.77.
- PET/CT imaging shows a lack of avidity at the T7 body with an SUV_{max} of 0.72.

Conclusion, Limitations, and Future Directions

- DCE-MRI perfusion plays an important role in detecting malignant spinal tumors when PET or biopsy are not available, and that DCE-MRI perfusion imaging should be performed in addition to PET/CT to improve the detection of spinal metastases that are not non-FDG avid and have SUVmax values below accepted diagnostic thresholds.
- Future directions include conducting analysis on more samples and incorporating the clinical judgment involved in assessing PET/CT imaging.
- Currently, the study measures the quantitative measures in DCE-MRI and PET and relates these measurements to the enhancement seen on corresponding imaging. In the clinical setting, there may be cases where SUVmax values may be below the accepted diagnostic thresholds of 2.5 and 4.0 reported in the literature but may possess enough qualitative avidity on a PET scan to alert a radiologist of suspicious metastases. Future studies can incorporate having multiple radiologists look at DCE-MRI and PET scans, observe for any intra-observer variability, and see how the quantitative guidelines for V_p and SUV_{max} seen in this study improve the detection of spinal metastases.

Disclosures

Deeptha Bejugam BS, Kyung K. Peck PhD, Atin Saha MD, Elena Yllera-Contreras MD, Onur Yildirim MD, Julio Arevajo-Perez MD PhD, Simone Krebs MD, Eric Lis MD, Sasan Karimi MD: None

Andrei Holodny MD: fMRI Consultants, LLC: Owner

4 Foolproof strategies

Edit
Avoid excess text

Design
Nice design-alignment

Font
Readability (Font sizes)

Free up
Don’t use boxes to separate sections

How to Begin

1. **Have a good idea of what you want your poster to look like- the order of items and where your images should go**

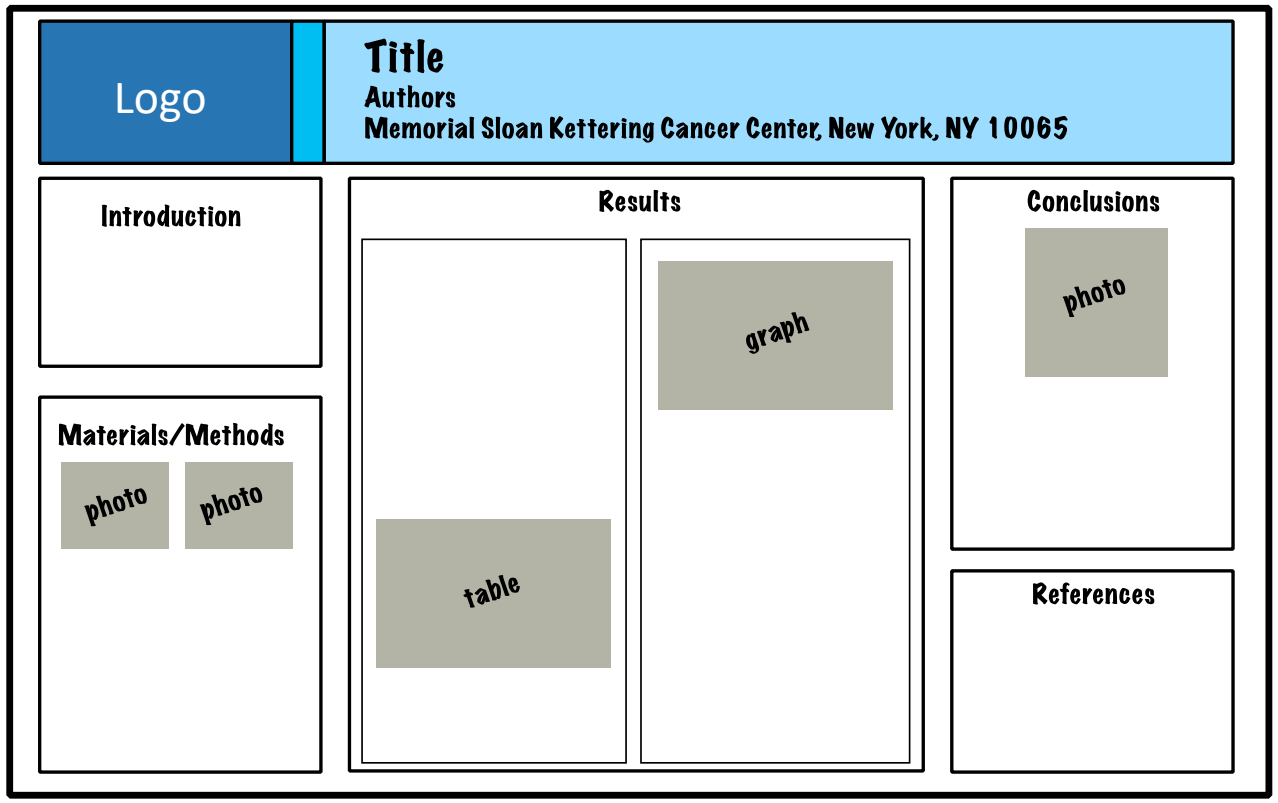

How to Begin

2. Familiarize yourself with PowerPoint.
Important tools to know are:

Text box

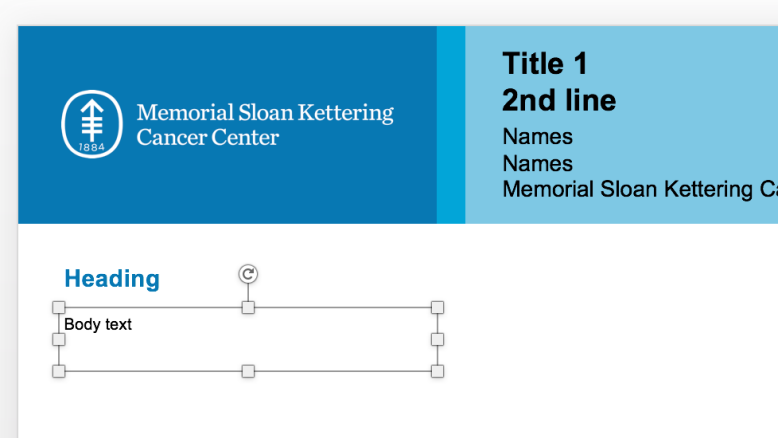

Insert tab

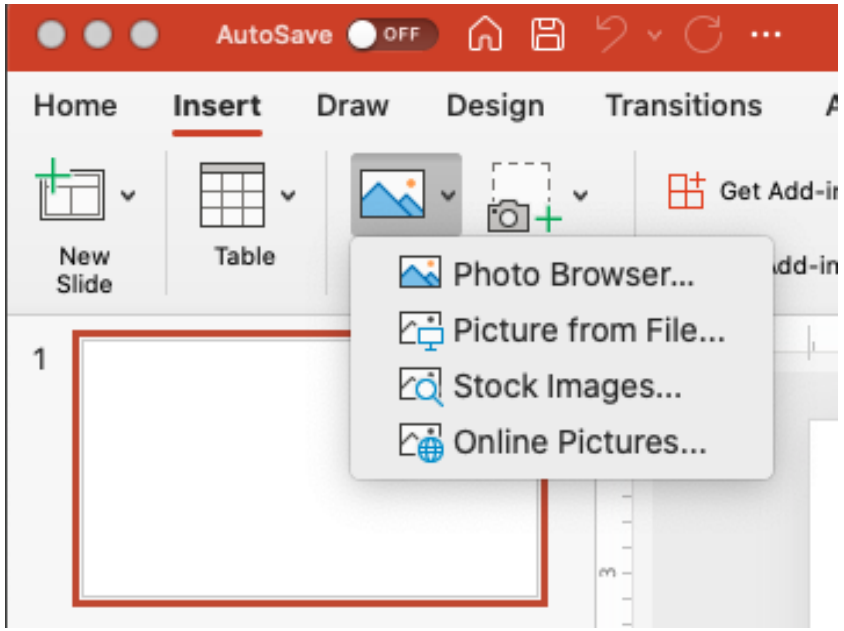

How to Begin

Arrange

Find it under the HOME Tab
Important for bringing items in front or behind others, grouping objects, or aligning them

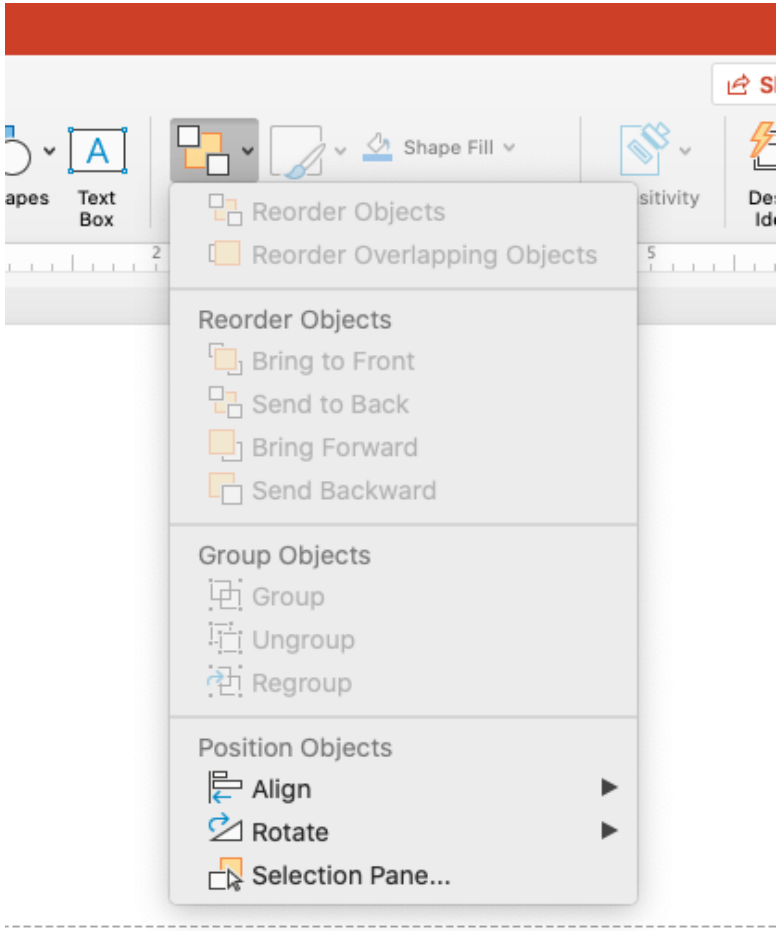

How to Begin

Zoom and Fit to Window

Find it under the VIEW Tab

Change your view in several preset increments. Fit to window is a quick way to see your entire poster at once.

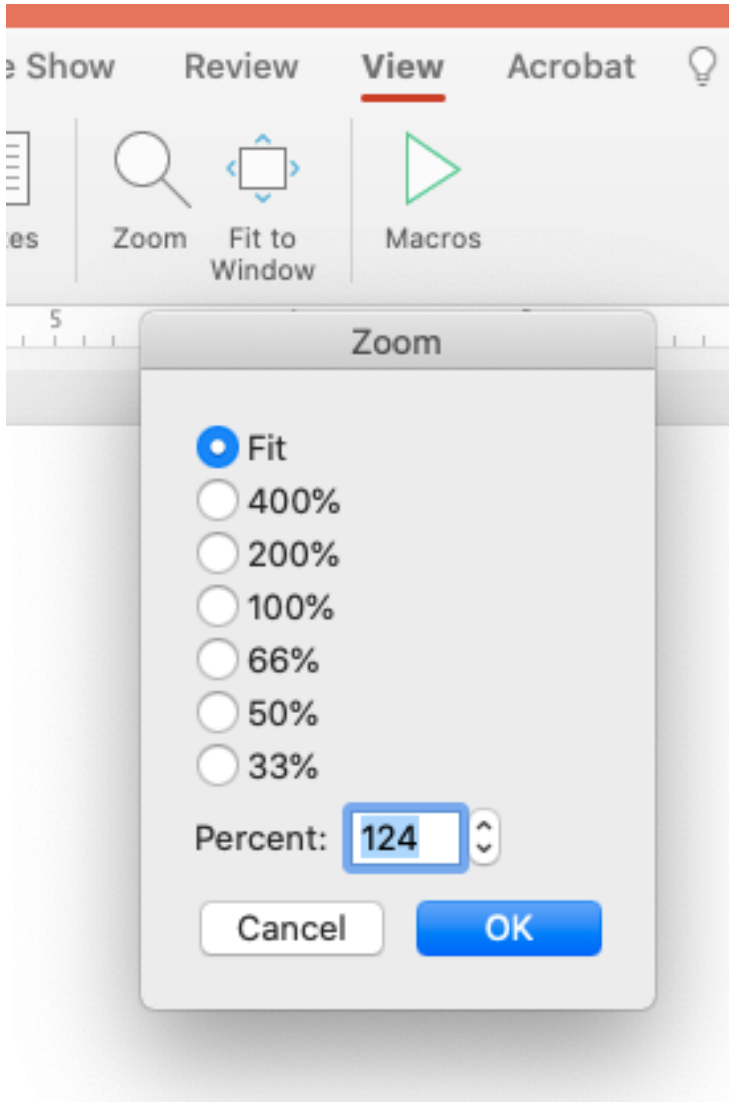

Poster Creation Process

STEPS

1. Gather all poster elements – text, graphics, images. Put them into a folder called, for example, “My Poster” saved to your HD
2. Open the prepared poster template
3. Copy your text to the template
4. Insert images
5. Move/resize elements as needed
6. Proofread
7. Create pdf of the poster

The Template

- You've been provided with a template, sized for MSK poster boards
- Template we provide are branded with appropriate:
  - MSK logo
  - MSK colors
  - MSK fonts

Some poster samples:

1

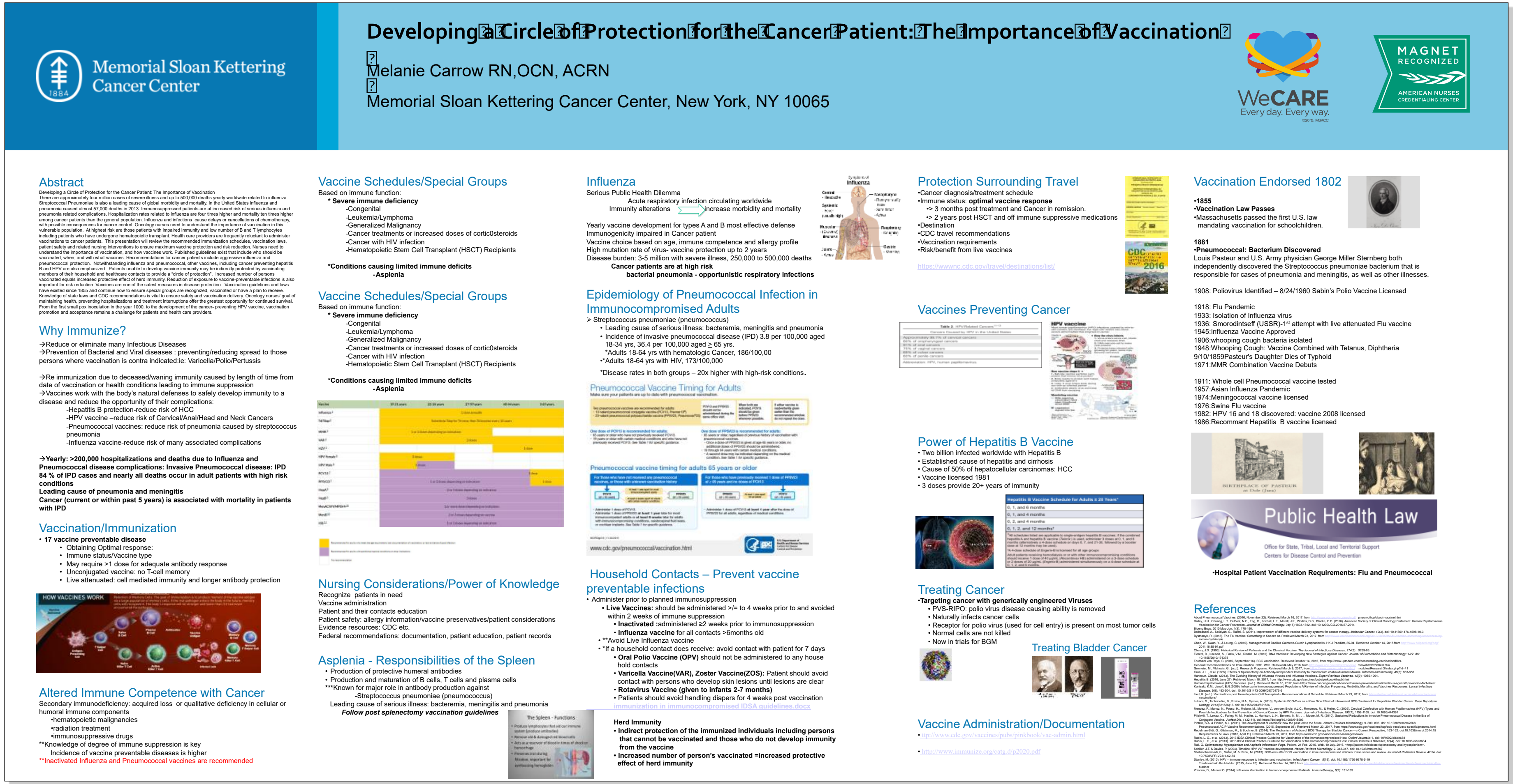

2

Memorial Sloan Kettering Cancer Center

Diagnosis and Treatment of Biliary Obstruction

DeeAnn Davidson AGACNP-BC, Cristy Fitzpatrick ANP-BC, Gloria Wong ACNP-BC, Kristen O'Hagan ANP-BC, Anita Schabel ANP-BC, Jennifer Flood ANP-BC
Memorial Sloan Kettering Cancer Center, New York, NY

Abstract

The purpose of this abstract is to provide a clinical overview of the possible causes of obstructive jaundice in order to facilitate the appropriate work up and treatment plan. Biliary obstruction refers to the blockage of bile flow from the liver to the small intestine. This blockage can occur at various levels in the biliary system. The major signs and symptoms are the result of bile not reaching its proper destination. Accumulation of bile leads to deposition of the skin (jaundice), conjunctival icterus, dark urine, pale stools and pruritus. The incidence of biliary obstruction is approximately 5 cases per 1000 people. The mortality and morbidity of obstructive jaundice is dependent on the cause. The most common causes of obstructive jaundice are: gallstones; neoplasms of the pancreas, gallbladder, bile duct and small intestine; pancreatitis; metastatic tumors to the lymph nodes in the porta hepatitis and benign bile duct strictures. Treatment of obstructive jaundice is based on both the cause and the anatomical location of the blockage. Proper evaluation includes: cross-sectional imaging, tissue pathology, invasive treatment modality, surgical consultation or staging where relevant. Nurse Practitioners (NPs) in all practice settings will encounter biliary obstruction. It is imperative that NPs have a comprehensive understanding of this complex medical condition. This enables proper diagnosis and treatment options based on the cause and the location of the obstruction which will improve clinical practice and patient outcomes.

Levels of Biliary Obstruction

1. Intrahepatic Bile Duct Obstruction

Causes: intrahepatic cholangiocarcinoma and sclerosing cholangitis

2. Perihilar Bile Duct Obstruction

Causes: gallbladder cancer, cholangiocarcinoma, gallstones, nodal disease from metastatic cancers

3. Distal Extrahepatic Duct Obstruction

Causes: gallstones, pancreatic cancer, duodenal cancer, cholangiocarcinoma of distal bile duct, ampullary cancer

Intrahepatic Biliary Obstruction Case Study

- 60 year old female presents to primary care doctor with 7 lb weight loss, severe pruritus, and painless jaundice
- Labs: Total Bilirubin (t bili) 13, Alkaline Phosphatase (alk phos) 432, AST 97, ALT 60, Creatinine 1.5, BUN 32, WBC 9
- Work up: Ultrasound of abdomen revealed dilated intrahepatic biliary ducts, common bile duct (CBD) measured 10mm, gallbladder wall normal and no gallstones identified
- Work up: patient admitted to hospital and IV hydration started for elevated Creatinine. Additional lab work including tumor markers (CEA, CA 19-9), PT/INR, Hepatitis B & C, repeat Hepatic Function, & Basic Metabolic. CT scan abdomen and pelvis with IV contrast performed once Creatinine corrected.
- CT scan of abdomen and pelvis revealed intrahepatic biliary dilation down to confluence of the common hepatic duct, dilated CBD, no focal liver lesions noted
- Patient underwent a percutaneous transhepatic cholangiogram and was noted to have a high bile duct obstruction. Interventional radiologist was able to cross the obstruction with internal/external biliary drain.
- Patient was referred for surgical evaluation

Intrahepatic Bile Duct Obstruction

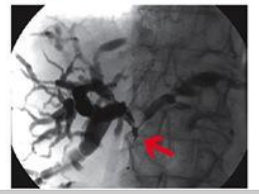

Placement of Internal/ External Biliary Catheter Through Intrahepatic Bile Duct Obstruction

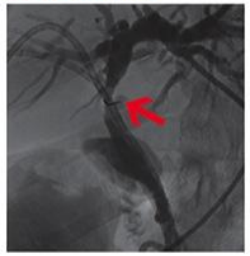

Cholangiogram Post Biliary Drainage

Levels Of Biliary Obstruction

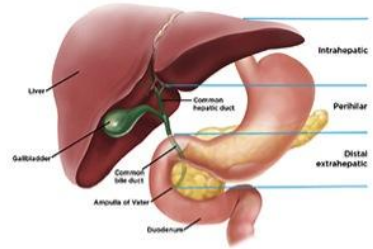

Perihilar Biliary Obstruction Case Study

- 57 yo male presents to primary care physician with nausea, abdominal pain, and jaundice
- Labs: WBC 8, T Bili 6, Alk Phos 248, AST 67, ALT 80
- Work up: Abdominal ultrasound revealed dilated intrahepatic bile ducts, CBD 12mm, gallbladder wall thickened with 3 cm mass noted within the gallbladder
- CT abdomen/pelvis with IV contrast revealed nodular gallbladder wall thickening with infiltrative margins with the adjacent liver parenchyma and 2.4cm x 2.3cm porta hepatis mass at the junction of right and left hepatic ducts.
- Work up: Tumor markers (CEA, CA19-9), PT-INR, Comprehensive panel
- Interventional radiology consult for biopsy and percutaneous biliary drainage/wall stent
- Brush biopsy of bile duct + adenocarcinoma consistent with pancreaticobiliary origin.
- Percutaneous primary biliary wall stent was placed across the obstruction
- Patient referred to medical oncology

Gallbladder Cancer Causing Perihilar Biliary Obstruction

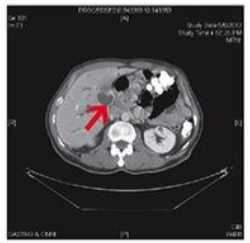

Perihilar Biliary Obstruction Caused by Gallbladder Cancer

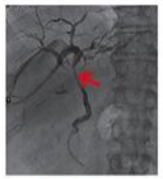

Wallstent Placement for Perihilar Biliary Obstruction

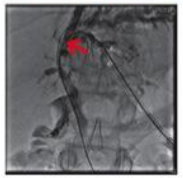

Distal Extrahepatic Bile Duct Obstruction Case Study

- 45 year old female presents to local ER with 2 day history abdominal pain and nausea/ vomiting
- Labs: WBC 13, T Bili 2.3, Alk Phos 123, AST 25, ALT 40
- Work up: Abdominal ultrasound reveals thickened gallbladder wall with pericholecystic fluid, multiple gallstones seen in the gallbladder, dilated CBD 10mm, positive Murphy's sign
- Gastroenterology (GI) consulted for acute cholecystitis

Distal Extrahepatic Bile Duct Obstruction Case Study

- Patient underwent endoscopic retrograde cholangiopancreatography (ERCP) & stone extraction. After sphincterotomy and stone extraction, the common bile duct was free of stones
- Patient was referred for surgical consult for elective cholecystectomy

Retained Common Bile Duct Stones Causing Extrahepatic Biliary Obstruction

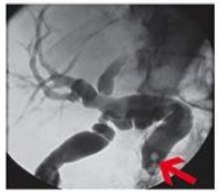

References

1. Blumgart LH, et al. *Surgery of the liver, biliary tract, and pancreas.* 4th ed. Saunders Elsevier; 2007.
2. de Groen PC, Gores GJ, LaRusso NF, et al. *Biliary Tract Cancers.* N Engl J Med 1999; 341: 1368.
3. Kavanagh PV, vanSonnenberg E, Wittich GR, et al. *Intervention-al Radiology of the biliary tract.* Endoscopy 1997; 29: 570
4. Lai EC, Mok FP, Tan ES, et al. *Endoscopic biliary drainage for severe acute cholangitis.* N Engl J Med 1992; 326: 1582
5. Nagorney DM, Donohue JH, Farnell MB, et al. *Outcomes after curative resections of cholangiocarcinoma.* Arch Surg 1993; 128: 871.
6. Nakeeb A, Pitt HA, Sohn TA, et al. Cholangiocarcinoma. *A spectrum of intrahepatic, perihilar, and distal tumors.* Ann Surg 1996; 224: 463.
7. Wu SM, Marchant LK, Haskal ZJ. *Percutaneous interventions in the biliary tree.* Semin Roentgenol 1997; 32: 228.

3

Experimental evaluation of MR-guided HIFU for ablation of sacroiliac joint using a model of human sacrum

Kathleen Jedruszczuk[1], Amitabh Gulati[2], Stephen Solomon[3], Elena Kaye[1]

1. Department of Medical Physics 2. Department of Anesthesiology 3. Department of Interventional Radiology, Memorial Sloan Kettering Cancer Center, New York, NY 10065

Background

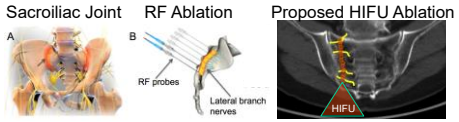

***Figure 1**. A. Sacroiliac joint is shown with an arrow. B. RF ablation of the lateral branches of the SIJ. C. Proposed noninvasive HIFU ablation of the lateral branch nerves.*

Chronic low back pain (CLBP) is a leading cause of work disability. In 15-30% of CLBP patients, the source is the dysfunction of the Sacroiliac Joint (SIJ) (1). One method providing therapeutic effectiveness is radiofrequency ablation (RFA) (Fig. 1), which is invasive and laborious procedure, limiting effective treatments for SIJ pain (2-3). HIFU could provide a non-invasive alternative by creating a continuous lesion lateral to the sacral foramina (Fig. 1C). The main risk of using HIFU for SI joint ablation is damaging sacral ventral nerve roots. A pilot study in swine demonstrated that MR-guided HIFU (MRgHIFU) ablation of SIJ is feasible, and lateral branch nerves can be ablated without damaging adjacent nerve roots (4). (Fig. 2)

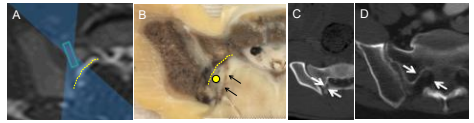

***Figure 2**. A. MR-guided HIFU of the SIJ in swine, the HIFU beam is shown in blue, muscle-bone interface (dashed line). E. Gross pathology showing the ablated zone (arrows) and the position of ablated nerve encompassed by it. C-D. Cropped CT images showing the difference between porcine and human sacra (same scale). Arrows point to dorsal foramina.*

The anatomy of human sacral foramina, however, is not identical to that of swine (Fig. 2). Hence, translating preclinical safety results into human patients may be prone to risk and further evaluation is needed.

THE PURPOSE of this study was to evaluate MRgHIFU ablation of SIJ in a model of human sacrum, specifically focusing on monitoring heating in the dorsal foramina.

Materials and Methods

Phantom: Images from an anonymized 67 yr. old female adult pelvic CT scan were used to segment the sacrum bone from adjacent muscle tissue. The segmented model was manufactured in a 3-D printer using (Acrylonitrile Butadiene Styrene) ABS plastic (5). The muscle tissue was mimicked by a high-temperature hydrogel matrix (gellan gum) combined with different sizes of aluminum oxide particles and other chemicals (6).

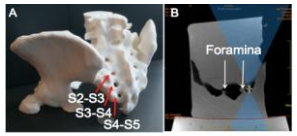

***Figure 3. A.** 3D printed sacrum model with relevant sacral spine segments labeled.*
***B.** MRI image of 3D printed sacrum in gel phantom with foramina labeled.*

Experiment: MRgHIFU experiment was performed using ExAblate 2000, a clinical HIFU system (InSightec, Ltd., Israel) installed in a 1.5 Tesla MRI scanner (GE Healthcare, USA). HIFU beam was applied as shown in Figure 3. All sonications were performed for 10 seconds at 1.00 MHz. Individual sonication parameters are listed in Table 1.

Results

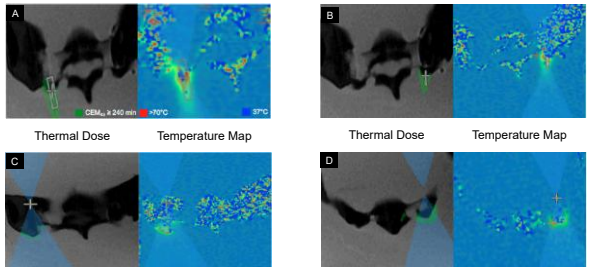

***Figure 4. Visualization of placing focal point on bone vs. behind bone (near-field approach) A**. Sonication #2 **B**. Sonication #5 **C**. Sonication #7 **D**. Sonication #8*
***A** and **B** both display the effect of placing the focal point on the bone, creating long lesions. **C** and **D** both display the effect of placing the focal point behind the bone, creating larger and wider lesions.*

Figure 4 shows representative examples of temperature rise and thermal dose during sonications targeting the approximate location of the lateral branch nerves, lateral to the foramina. Table 1 summarizes the maximum temperatures that were measured in the target location and at the opening of the dorsal foramina. In 2 out of 9 locations, elevated temperature in the foramina resulted in lethal thermal dose extending into foramina. These regions were always immediately adjacent to the bone, and did not propagate beyond the posterior part of the foramina.

Sonication #	Location	Acoustic Energy, J	Acoustic Power, W	Target Temp, C	Foramen Temp, C	Lethal Dose at foramen ?
1	L-S4-5	1259	129	84	52	Yes
2	L-S3-4	1392	147	108	39	No
3	R-S3-4	1049	112	101	42	No
4	L-S4-5	1005	107	72	53	Yes
5	R-S1-2	1031	109	86	45	No
6	R-S4-5	1009	107	80	45	No
7	L-S1-2	1006	106	83	42	No
8	R-S3-4	1060	108	97	40	No
9	R-S2-3	1050	107	71	42	No

Discussion

The sacrum phantom, presented here, enabled preliminary evaluation of MRgHIFU application for non-invasive treatment of SIJ low back pain. While this phantom does not model the effects of perfusion, which would reduce the temperature rise that was observed here, it provides realistic geometry and dimensions of the sacrum that can help optimize the targeting strategy. Positioning of the HIFU focus in relation to the sacral foramina and sacral bone need to be studied to determine a protocol which delivers lethal thermal dose to the target location between the SIJ and the foramen, while preventing undesired heating inside the foramen and minimizing the damage of adjacent muscle.

Take Home Message

In order to safely apply this method in a clinical setting, the strategy of maintaining control over damage in the lateral to medial range needs to be optimized. Preventing heating of sacral foramina and minimizing muscle damage is crucial to the safety of this procedure.

Acknowledgments

FUS Foundation Global Internship Program, Office of Faculty Development at Memorial Sloan Kettering Cancer Center and Paul Booth for assistance with 3D printing, Shimon Kraler, Jacob Chen, Neha Dhawan (InSightec Ltd) for technical support.

References

1. Cohen SP. *Anesthesia & Analgesia. 2005.*
2. Yin W, et al. *Spine.* 2003.
3. Roberts SL, et al. *Regional anesthesia and pain medicine.* 2014.
4. Kaye E., et al. Presented at ISTU 2016, Tel Aviv.
5. Menikou G., et al. *Ultrasonics. 2015.*
6. King R., et al. *IEEE Trans Ultrason Ferroelectr Freq Control. 2011.*

Poster Elements

Title- largest element across top

- Largest font- Recommend using all caps

Subheadings:

- ***Abstract (optional)-*** some meetings require one
- **Introduction/Background**
- **Methods**
- **Results**
- **Conclusions**
- ***Future Directions/Discussion***

Body text

Graphs, photos, tables

Layout

Aim for a MAX of about 800 words on your poster

Less is More!!
Tell your story with images

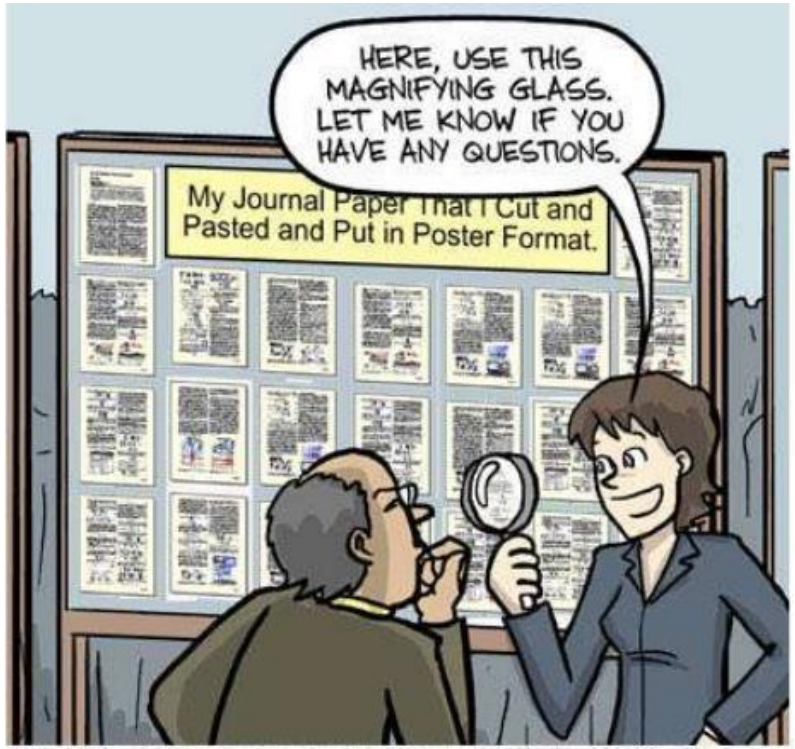

Doumont, J., *English Communication for Scientists*. Cambridge, MA: NPG Education.

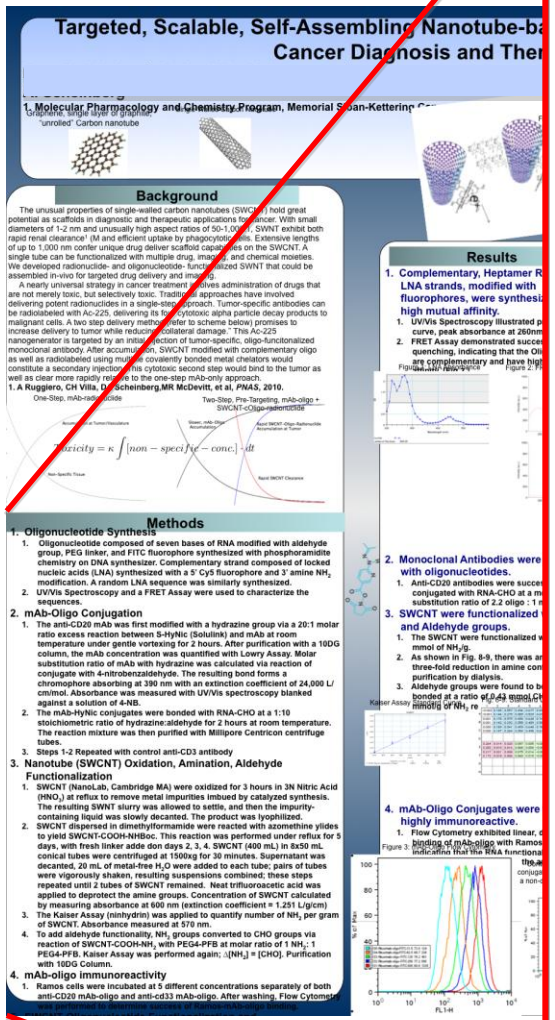

Methods

1. Oligonucleotide Synthesis

1. Oligonucleotide composed of seven bases of RNA modified with aldehyde group, PEG linker, and FITC fluorophore synthesized with phosphoramidite chemistry on DNA synthesizer. Complementary strand composed of locked nucleic acids (LNA) synthesized with a 5' Cy5 fluorophore and 3' amine NH_2 modification. A random LNA sequence was similarly synthesized.
2. UV/Vis Spectroscopy and a FRET Assay were used to characterize the sequences.

2. mAb-Oligo Conjugation

1. The anti-CD20 mAb was first modified with a hydrazine group via a 20:1 molar ratio excess reaction between S-HyNic (Solulink) and mAb at room temperature under gentle vortexing for 2 hours. After purification with a 10DG column, the mAb concentration was quantified with Lowry Assay. Molar substitution ratio of mAb with hydrazine was calculated via reaction of conjugate with 4-nitrobenzaldehyde. The resulting bond forms a chromophore absorbing at 390 nm with an extinction coefficient of 24,000 L/cm/mol. Absorbance was measured with UV/Vis spectroscopy blanked against a solution of 4-NB.
2. The mAb-HyNic conjugates were bonded with RNA-CHO at a 1:10 stoichiometric ratio of hydrazine:aldehyde for 2 hours at room temperature. The reaction mixture was then purified with Millipore Centricon centrifuge tubes.
3. Steps 1-2 Repeated with control anti-CD3 antibody

3. Nanotube (SWCNT) Oxidation, Amination, Aldehyde Functionalization

1. SWCNT (NanoLab, Cambridge MA) were oxidized for 3 hours in 3N Nitric Acid (HNO_3) at reflux to remove metal impurities imbued by catalyzed synthesis. The resulting SWNT slurry was allowed to settle, and then the impurity-containing liquid was slowly decanted. The product was lyophilized.
2. SWCNT dispersed in dimethylformamide were reacted with azomethine ylides to yield SWCNT-COOH-NHBoc. This reaction was performed under reflux for 5 days, with fresh linker adde don days 2, 3, 4. SWCNT (400 mL) in 8x50 mL conical tubes were centrifuged at 1500xg for 30 minutes. Supernatant was decanted, 20 mL of metal-free H_2O were added to each tube; pairs of tubes were vigorously shaken, resulting suspensions combined; these steps repeated until 2 tubes of SWCNT remained. Neat trifluoroacetic acid was applied to deprotect the amine groups. Concentration of SWCNT calculated by measuring absorbance at 600 nm (extinction coefficient = 1.251 L/g/cm)
3. The Kaiser Assay (ninhydrin) was applied to quantify number of NH_2 per gram of SWCNT. Absorbance measured at 570 nm.
4. To add aldehyde functionality, NH_2 groups converted to CHO groups via reaction of SWCNT-COOH-NH_2 with PEG4-PFB at molar ratio of 1 NH_2: 1 PEG4-PFB. Kaiser Assay was performed again; $\Delta[NH_2] = [CHO]$. Purification with 10DG Column.

4. mAb-oligo immunoreactivity

1. Ramos cells were incubated at 5 different concentrations separately of both anti-CD20 mAb-oligo and anti-cd33 mAb-oligo. After washing, Flow Cytometry was performed to determine success of Ramos-mAb-oligo binding.

Layout – Fonts

Serif vs Sans Serif

Georgia

Flourishes adorn the lettering

Arial

Clean, straight lines
Without pointy tails

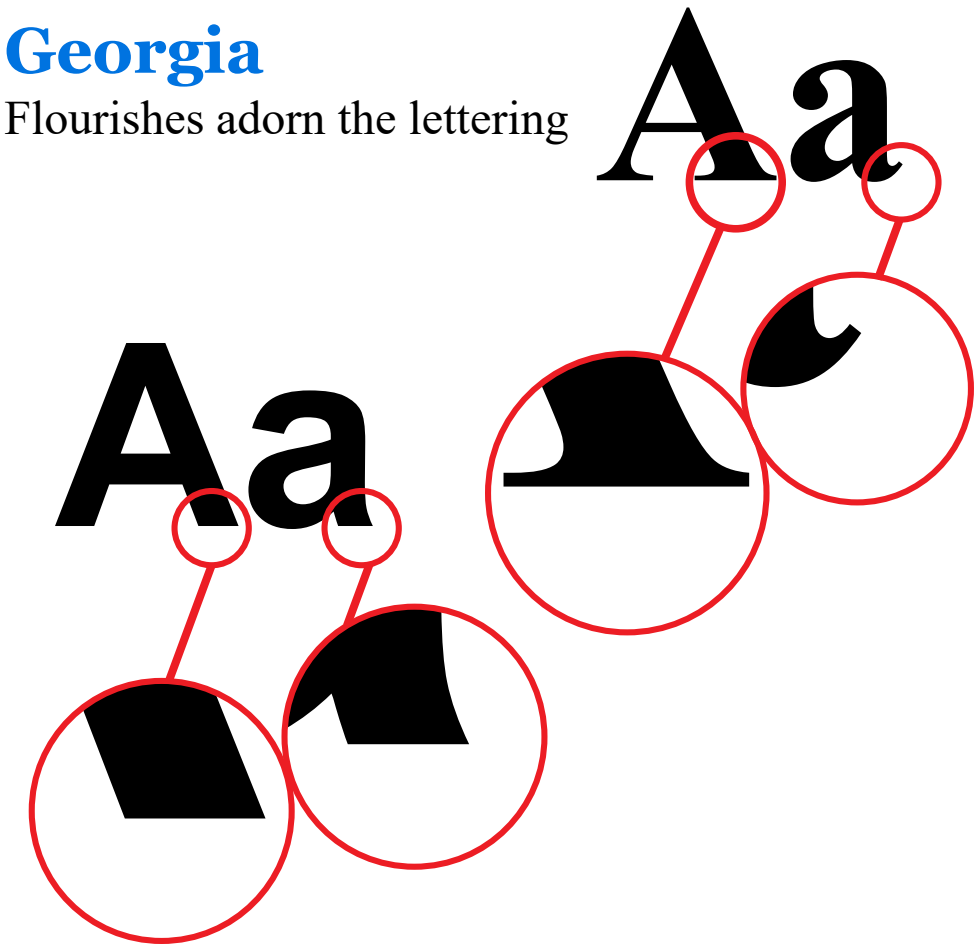

Layout – Fonts

- MSK Fonts: **Arial, Georgia, Open Sans**

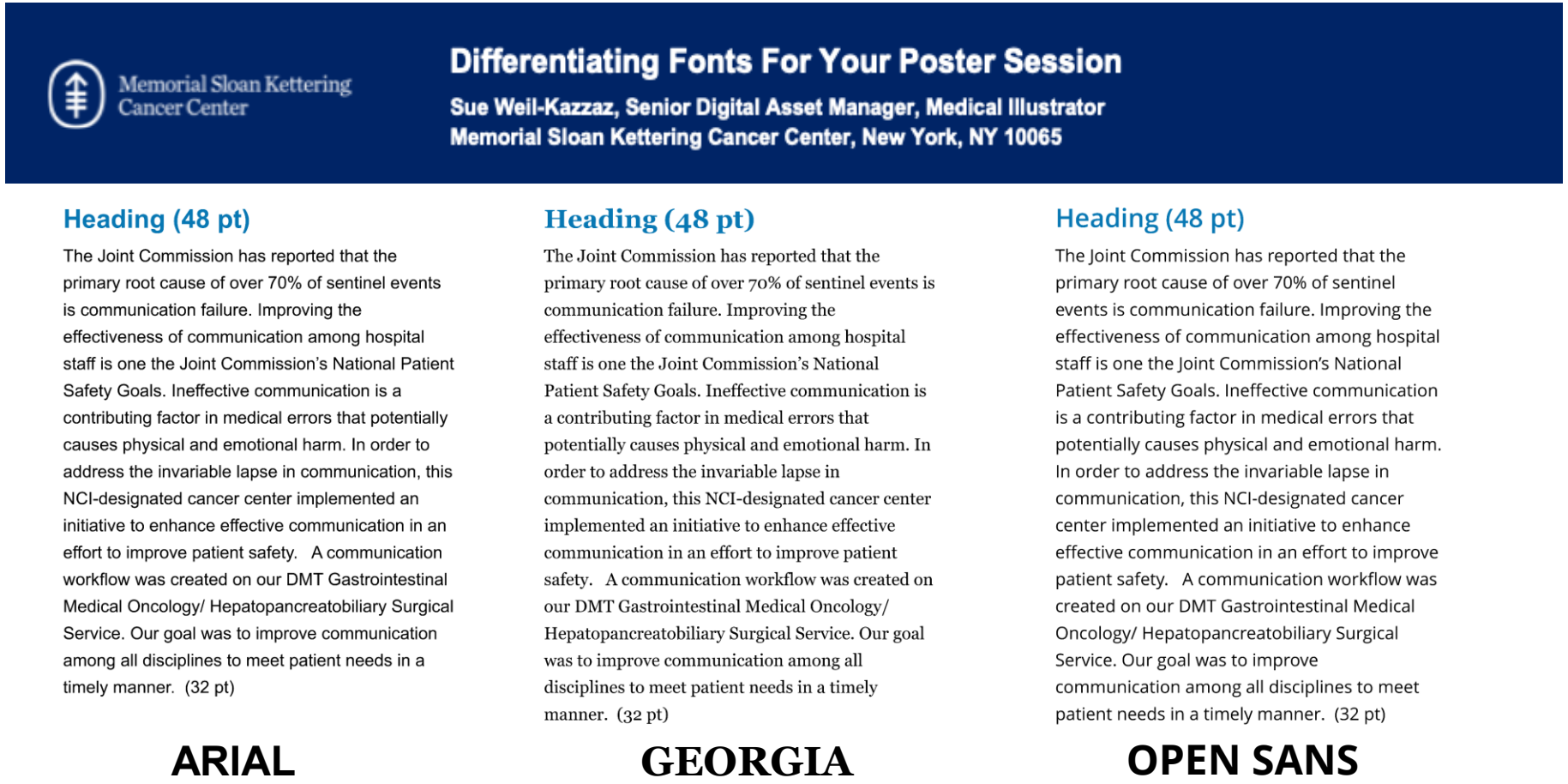

Layout – Fonts

- **Size**
  - **Title – Largest Font, all caps?**
    60-120 pts
  - **Subheadings (Results, Concl, etc)**
    24-48 pts
  - **Body text: 18-36 pts**
  - **Captions: ≥ 18 pts**

Does it look right on your PPT page

- Try not to use a font size less than 18 pt.
- All subtitles should be the same size, all captions (if used) under images should be the same size, all body text should be the same size
- You may need to adjust font sizes when you've added all elements to make items fit and/or best use the poster space.

Layout – Fonts

Never use

COMIC SANS!!!

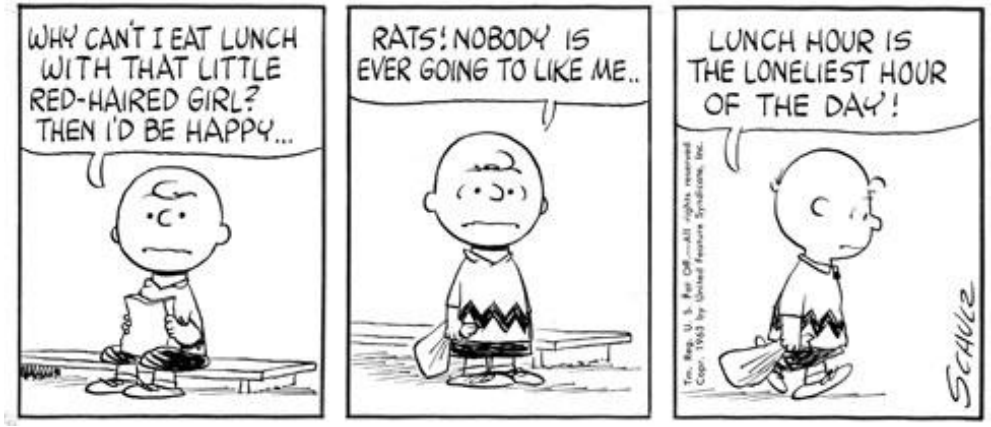

Your data is too important

Layout

What about the Logo?

Memorial Sloan Kettering Cancer Center

Don’t:

- Stretch it in any direction
- Change the color
- Add another logo to it
- Separate the words from the symbol

"Click" Chemistry for the Radiosynthesis of Fluorine-18 Labeled pH (Low) Insertion Peptide (pHLIP) PET Tracers for the pH-Sensitive Targeting of Acidic Tumor Tissue

1)Molecular Pharmacology and Chemistry Program and the Department of Radiology, Memorial Sloan-Kettering Cancer Center, New York, New York, NY 10065, USA.
2)Department of Physics, University of Rhode Island, Kingston, RI 02881USA.

Introduction: pHLIP for Tumor Imaging

pHLIP (pH low insertion peptide) is the term for a variety of water soluble peptides with an amino acid sequence allowing for the selective insertion into cell membranes based on the pH of the extracellular environment.

WT-pHLIP with 37 amino acids, bearing two aspartic acid residues, changes its conformation at a pH < 7 due to the protonation of the two aspartic acids. The resulting change in lipophilicity of the pHLIP under acidic conditions allows for the insertion of the peptide across the cell membrane as an α-helix (state III). The N-terminus was shown to remain extracellular while the C-terminus will reach the intracellular cavity in the case of full insertion. At physiologic pH (pH 7.4), however, pHLIP displays a transient interaction with cell membranes at extracellular pH ≥ 7 (state I and II).

pH-dependent insertion of pHLIP across cell membranes:

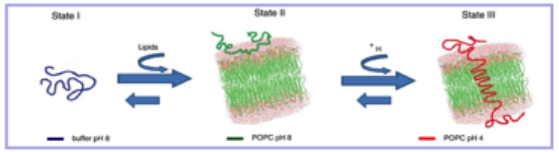

M. Musial-Siwek et al. / Biochimica et Biophysica Acta 1798 (2010) 1041–1046

The acidity of the tumor microenvironment is a known part of the pathology of many cancers mainly due to

Methods: Two-step Radiosynthesis of [^{18}F]-Labeled pHLIP Derivatives

Acidohexanoic acid derivatized pHLIP analogues of WT-pHLIP and short-3E were used for the establishment of a two-step [^{18}F]-labeling protocol for the relatively large (MW of ca. 3000 to 4500 g/mol) pHLIP peptides. A novel prosthetic group, fluoropyridinealkyne (**3**), was designed for the fast and efficient Huisgen „click" coupling of the fluorine bearing small molecule to the desired peptide. The non-radioactive prosthetic group (**3**) was synthesized starting from fluorobromopyrdine (**1**) and Sonogashira coupling to TBS-protected ethyne followed by deprotection with TBAF. The advantage of the slightly volatile Fpyralkyne (**3**) is its small size designed for little affection of the properties of the peptide and its UV-visibility. Prosthetic group (**3**) was successfully utilized for the synthesis of non-radioactive Fpyralkyne peptide standards of WT-pHLIP and short-3E in both the L- and D-configuration.

Synthesis of the fluorinated prosthetic group (3) for the cold "click" to azido-pHLIP

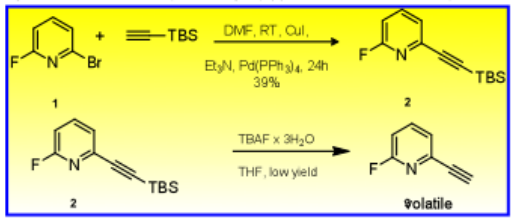

pHLIP analogues with varying length and amino acid sequence:

Name AA: amino acid	Amino Acid Sequence		
	N-Terminus	transmembrane sequence	C-Terminus
WT-pHLIP (37 AA)	ACEQNPIY	WARYADWLFTTPLLLDLALLV	DADEGT
Fast1	ACEDQNPY	WARYADWLFTTPLLLLDLALLV	DG
Fast2	ACEDQNPY	WRAYADLFTPKTLLDLLALW	DG
Short-1D	ACEDQNP	WARYADLLFPTTLAW	
Short-1E	ACEEQNP	WARYAELLFPTTLAW	
Short-2D	ACEDQNP	WARYADWLFPTTLLLLD	
Short-2E	ACEEQNP	WARYAEWLFPTTLLLLE	
Short-3E (25 AA)	ACEEQNP	WARYLEWLFPTETLLLEL	

Radiosynthesis of [^{18}F]-labeled pHLIP analogues: first step [^{18}F]-labeling of an alkyne bearing prosthetic group: Bromoprecursor (**4**) was used as the starting material for the synthesis of [^{18}F]-3. Reaction

From "Pimp My Poster," Daniel Ciznadija

On Both Sides????

NO!

Impact of the Spinal Cord Injury Rehabilitation Evidence (SCIRE)

[1]Lawson Health Research Institute, London, ON; [2]University of Western Ontario, London, ON;
[3]GF Strong Rehabilitation Centre, Vancouver, BC; [4]University of British Columbia, Vancouver, BC

What is SCIRE?

The Spinal Cord Injury Rehabilitation Evidence (SCIRE) is a synthesis of the research evidence underlying outcome measures and rehabilitation interventions to improve the health of people living with spinal cord injury (SCI). This project is intended to translate existing knowledge best clinical practice. This research synthesis also informs relevant decision-making in public policy and practice settings applicable to SCI rehabilitation.

SCIRE is available via book, CD and online format at www.icord.org/scire[1]

Assessing Impact

The Becker Medical Library Model for Research Impact was utilized in order to assess SCIRE's impact.[2] This Model tracks research impact at four levels:

Stage 1: Research Output

SCIRE is distributed through a free website and CDs.

Dissemination has been through various products:

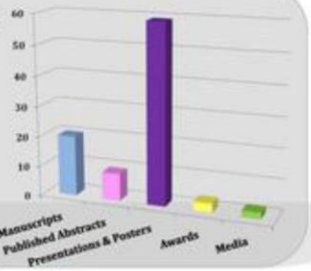

Stage 2: Knowledge Translation*

SCIRE's h-value	3
SCIRE's m-value	1.5
Total No. of Cited References	26
Total No. of Reprints Requested	4
Total Website Hits	353,341
Website Hits per Day	604
Used by Other Studies	3
Used by Canadian Working Groups	3

* since 2007

Stage 3: Clinical Implementation

- By front-line clinicians to teach other front-line clinicians best practice at Parkwood hospital.
- By SCI rehabilitation program director at Parkwood

Future Developments

Standards of Care	Knowledge Translation	Research Priorities
Standards of Care and Guidelines	Clinical Guidelines	Consensus Research Priority Setting
Outcome Measure Standardization	Implementation of Best Evidence	Strategic funding based on Research Priority Setting
Models of Care	SCI Case Studies	
Policy Implications	Educational Modules	
	Multiple Publications	

Spinal Cord Injury Rehabilitation Evidence

Summary

- SCIRE has combined the efforts of expert scientists, clinicians, consumers and stakeholders to increase the accessibility of quality information in SCI rehabilitation.
- SCIRE provides a comprehensive research synthesis, focusing on treatment interventions and outcome measures in SCI rehabilitation across the continuum of care.
- Future editions will continue to update, improve and add new topics to facilitate moving research from the benchside to the bedside and community.
- SCIRE should improve health for Canadians by keeping healthcare professionals, scientists, policy-makers and consumers with SCI updated about the evidence.

References

1. Eng JJ, Teasell RW, Miller WC, Wolfe DL, Townson AF, Hsieh JTC, Konnyu KJ, Connolly SJ, Foulon BL, Aubut JL, editors. SCIRE: Spinal Cord Injury Rehabilitation Evidence. Version 2. Vancouver. Available at:

From "Pimp My Poster," Daniel Ciznadija

Layout - Images

- Increase effectiveness
- Catches the reader's eye
- Communicates message faster
- Helps reader retain information
  - Use best images you have
  - Images are focal point, not filler
  - Images with contrast draw more attention

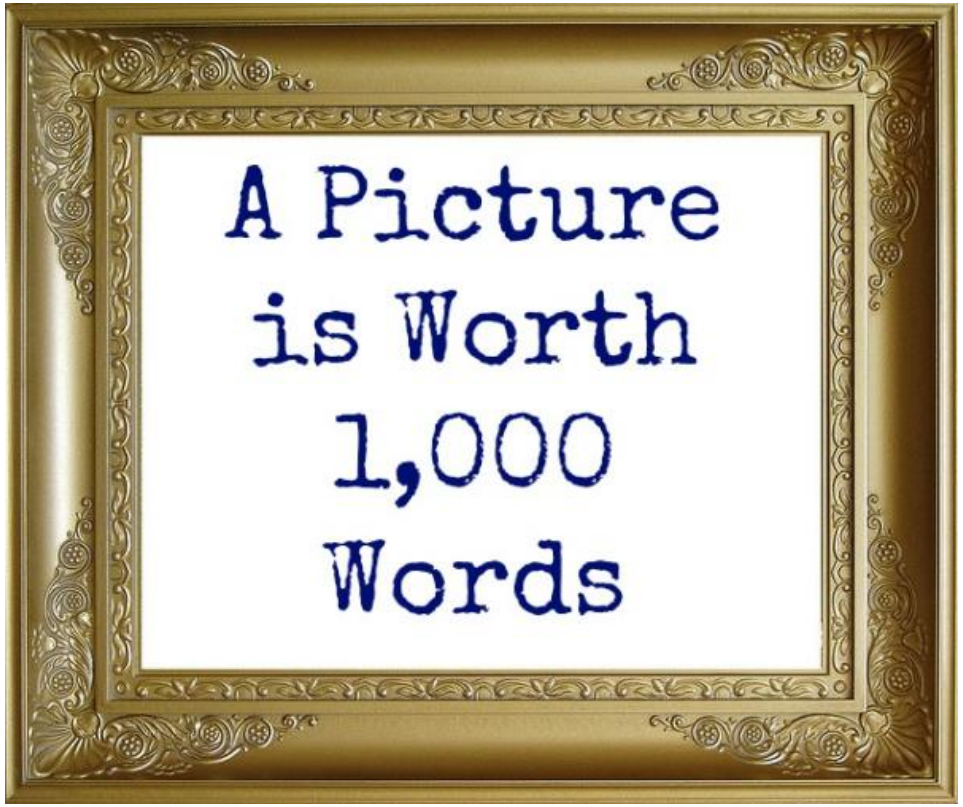

Layout - Images

Be careful using images from the internet

- **copyright issues** – always check!
  Seek permission when in doubt
- jpg, tiff, png, pdf
- **crop** to focus attention and eliminate unnecessary information
- Best resolution to use is **between 150 but no more than 300 dpi**
- Low resolution images on your poster are blurry/pixelated (zoom in 300% or more to test)

Layout - Images

Where to find them:

1. **MSK Digital Asset Library-**
   http://digitalassets.mskcc.org/

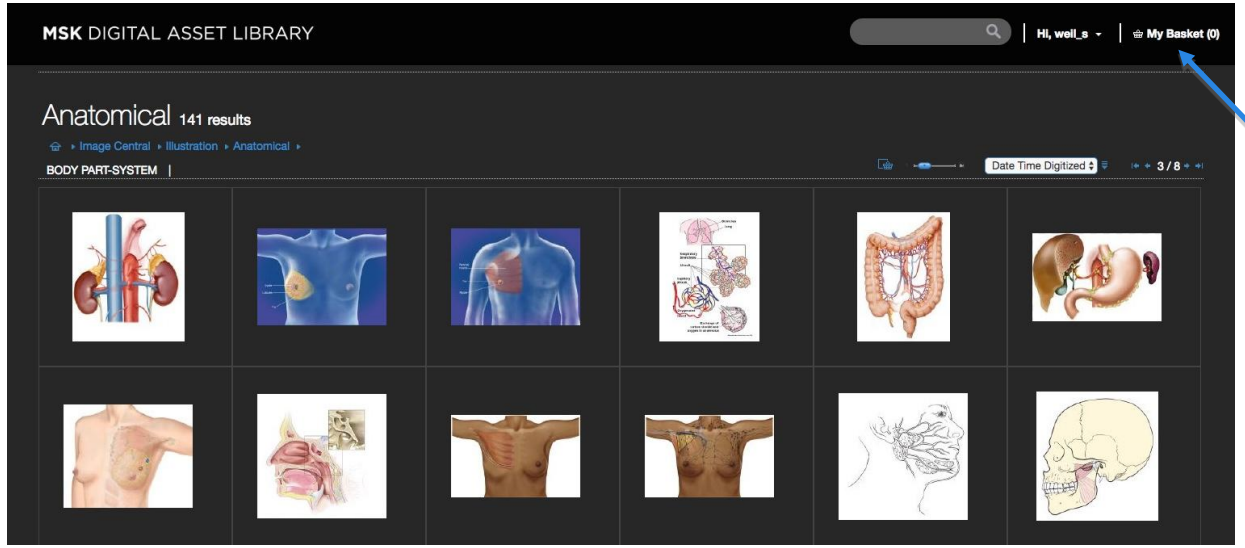

- Photos- head shots, facilities, events, historical, scientific, stock
- Illustrations
- Animations

1. Click on an image
2. Place it in your order basket
3. Open your basket
4. Click on the "Request Images" button Request images
5. Tell us you're using it for a poster session and hit the "Save" button
6. You'll receive your image via email within 24 hours.

Layout - Images

Where to find them:

2 Stock

- iStock- https://www.istockphoto.com
- Science Source- https://www.sciencesource.com

Design and Creative Services has accounts with these stock houses.
Visit the site(s) and note the image file #s. Forward to Design and Creative Services and we will purchase the image for you.
There will be a charge to your cost center.

Layout - Images

Where to find them:

3 Internet

- Assume all online images are protected by copyright- you may find the copyright holder contact info on the image and can ask for permission. You CAN use Creative Commons images- https://search.creativecommons.org/

- The dpi (pixel count) is important. Zoom in 300% or more to see if the image is blurry or pixelated.

Layout - Images

Where to find them:

4 Use your own

- Take your own photos- make sure the lighting is good and resolution is at least 150 dpi. Bring into an image editing program (Photoshop) if you need to make adjustments to lighting, cropping, color.
- Insert graphs, tables, diagrams that you have created.

5 Commission Design and Creative Services

Call or email the Design and Creative Services office (125-1440 or graphics@mskcc.org) and we can set up a photoshoot or illustrate the image you need.
There is a charge to your cost center.

Layout – Inserting Images

Insert a picture from your computer on your slide

1. Click where you want to insert the picture on the slide.

2. On the **INSERT** tab, in the **Images** group, click **Pictures**.

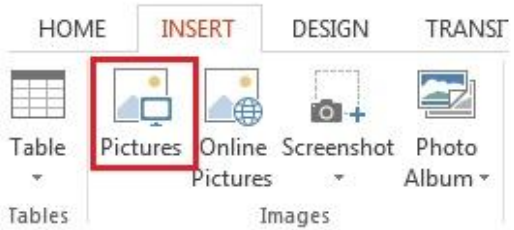

3. In the dialog box that opens, browse to the picture that you want to insert, click that picture, and then click **Insert**.

> **Tip:** If you want to insert multiple pictures at the same time, press and hold the Ctrl key while you select all the pictures you want to insert.

Layout - Effective Graphs

Graphs:

- If possible, avoid using colored backgrounds

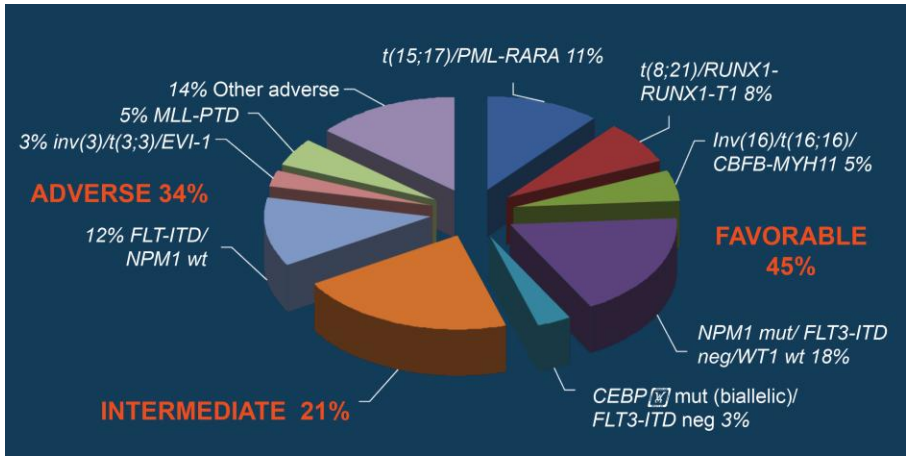

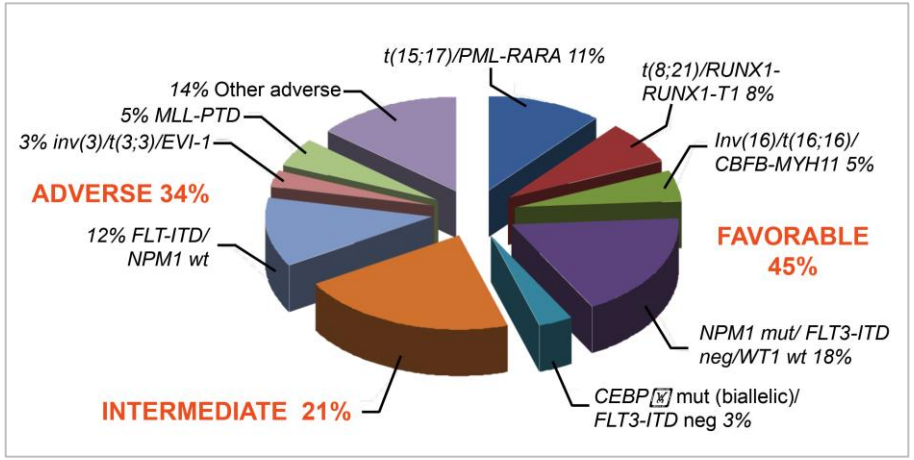

- Give your graphs clear and concise titles- make your graphs easily understood by the viewer.

- Avoid using acronyms or abbreviations unless they are widely used by your audience.

Layout - Effective Graphs

Graphs:

- Avoid gridlines and backgrounds

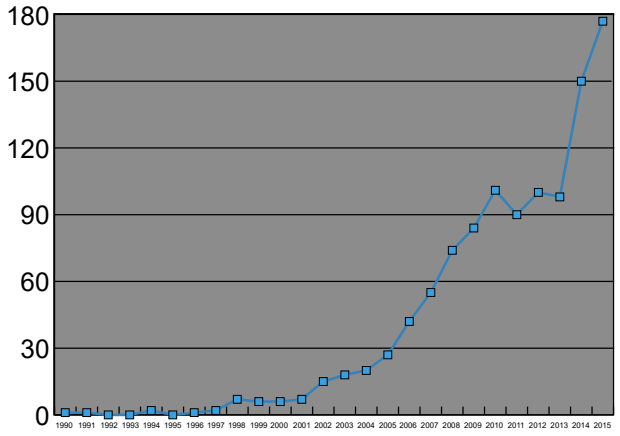

BAD

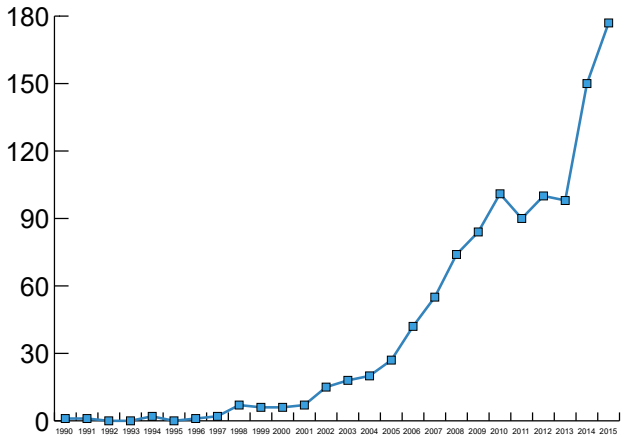

GOOD

- Gray background doesn't add anything
- Viewing on a monitor, your audience is more interested in seeing a trend than exact data values

Layout – Effective Graphs

Graphs:

- 3-D can confuse your audience

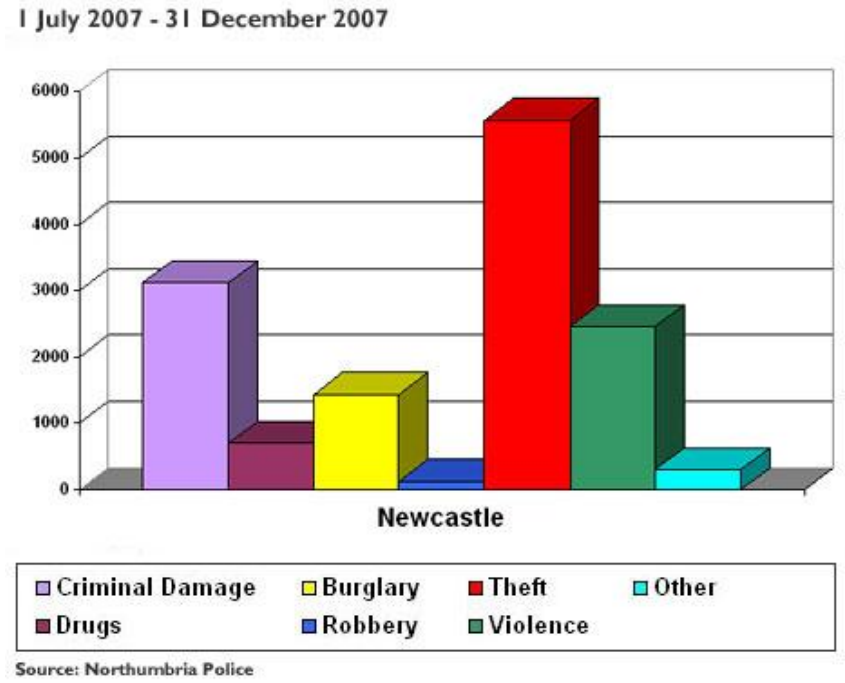

Layout

Color and background – **Less is more!**

Color

- Light backgrounds
  with dark text (printing)
- No flourescent colors
- Bad combinations:
  - red or black on blue
  - any color on red
  - yellow on white
  - text and background
    are similar

Backgrounds

- be wary of templates
- Not too busy
- Distracting pics

Poster P-139

Development of SKI242, an inhibitor of the resistant cell line H1975 of non-small cell lung cancer, for use as a pharmacokinetic tracer

Background

Non-small cell lung cancers (NSCLC) have been responding to treatment with aminoquinazoline based tyrosine kinase inhibitors. Tumours that have an L858R mutation in the kinase domain (NCI-H3255) are especially susceptible to treatment, these tumours often acquire a secondary mutation T790M (NCI-H1975) which renders them resistant to the amino quinazoline inhibitors. The goal of the study is to develop a radiotracer that is able to non-invasively image resistant NSCLC tumours.

Recently it was shown that certain bromo-aminoquinazoline based analogs were able to inhibit even the resistant strain of NSCLC[1,2]. These analogs were substituted α,β-unsaturated side chain making it a good michael acceptor which would react with a Cys-797 in the active pocket to make a covalent bond. A co-crystal structure of PD168393 and the ATP binding site of EGFR was solved by Blair J.A, *et-al*[3] confirming the existence of a covalent bond between the β carbon of the side chain and the sulfur of Cys 797.

[1] Sos M.L. *et-al*, (2010), Cancer Research, 70(3), 868-874, [2] Pawar V.G. *et-al*, (2010), J of Med. Chem., 53, 2892-2901, [3] Blair J.A. *et-al* (2007), Nat. Chem. Bio., 3(4), 229-238

Methods

A series of analogs were synthesized to be tested, PD16893 (AG09024), the iodo analog (SKI-242) of PD16893, an EGFR inhibitor SKI-243 and the bromine analog of SKI-243 (AG09094). SKI-243 has been shown in our lab to bind to NCI-H3255[1]and to A431 cells, both of which express EGFR. The ability of the analogs to inhibit cell growth was confirmed using MTT assays. The analogs showed different proliferation profiles in the 2 lung cancer cells lines. Using the radiolabeled analog of SKI-242 standard in vitro displacement studies were conduct to verify that binding was competitive and that they could be displaced. A PET study was performed using ^{124}I-SKI242 as well as a biodistribution study to further confirm our PET data.

[1] Medina O.P. *et-al*, 149(3), (2010), J of Controlled Release, 292-298.

Synthesis

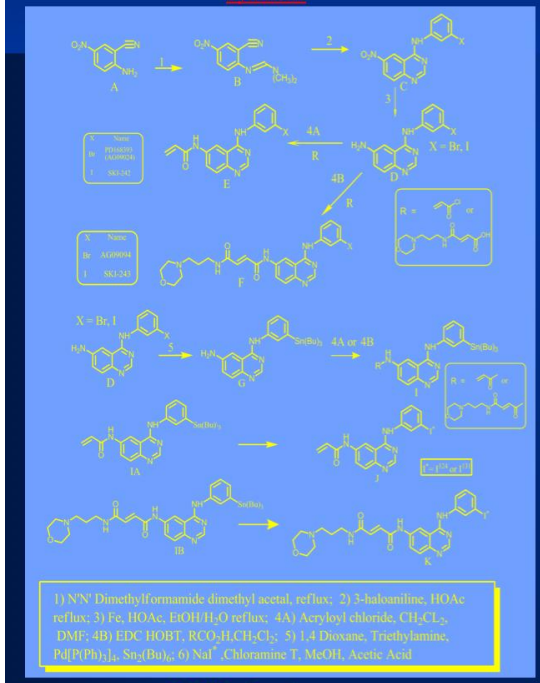

1) N^{1}N^1 Dimethylformamide dimethyl acetal, reflux; 2) 3-haloaniline, HOAc reflux; 3) Fe, HOAc, EtOH/H_2O reflux; 4A) Acryloyl chloride, CH_2CL_2, DMF; 4B) EDC HOBT, RCO_2H,CH_2Cl_2; 5) 1,4 Dioxane, Triethylamine, $Pd[P(Ph)_3]_4$, $Sn_2(Bu)_6$; 6) NaI^*,Chloramine T, MeOH, Acetic Acid

Proliferation Assays

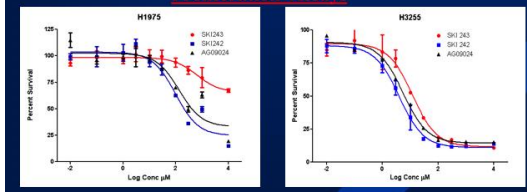

Displacement Assays

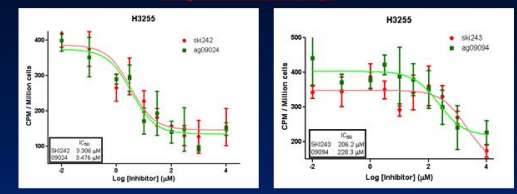

Biodistribution Data

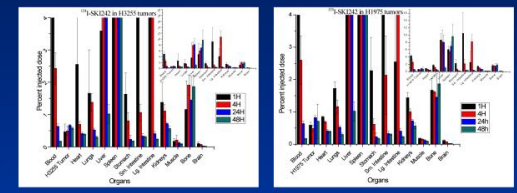

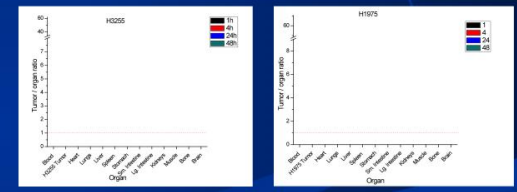

PET Images

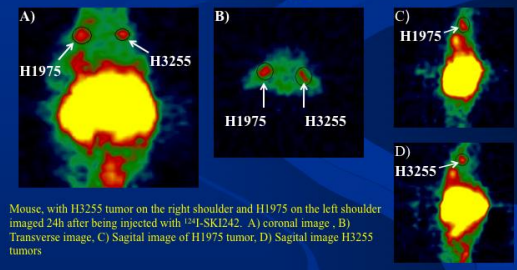

Mouse, with H3255 tumor on the right shoulder and H1975 on the left shoulder imaged 24h after being injected with ^{124}I-SKI242. A) coronal image , B) Transverse image, C) Sagital image of H1975 tumor, D) Sagital image H3255 tumors

Conclusion

- The 4 EGFR inhibitors were synthesized as well as the tin precursors.
- The tin precursors were radiolabeled with either I^{124} or I^{131}
- The ability of the iodo and bromo analogs to inhibit proliferation of different lung cancer lines, was validated using MTT assays.
- Using the radiolabeled analogs we were able to conduct *in-vitro* displacement assays by incubating with varying concentrations of the cold ligand.
- PET studies were conducted using ^{124}I-SKI242, the animals were later euthanized and the organs were harvested so that the PET images could be confirmed with the biodistribution study.
- Tumor uptake of the tracer is observed in both the resistant and sensitive cell lines. The percent injected dose per gram could be improved upon, but the ability to image a resistant cell line is the major accomplishment of this study. The tumor to organ ratios at the 24 and 48 hour time points are favorable for most organs

Acknowledgments

Ludwig Institute for Cancer Research ,Small Animal Imaging Facility MSKCC,

Radio Chemistry / Cyclotron Core MSKCC

Layout

- Use **bullets** rather blocks of text
- Use **italics** or **Bold**

- **Proofread!!**
  - correct spelling
  - avoid spacing errors within or between words

Finishing your Poster

Proofread before submitting to be printed

1. Make a pdf
2. Submit to the GME office for printing

Presenting your Poster

Your poster is a tool designed to:

1) Gain the interest of the viewer

2) initiate discussion

The word present is key

You should present yourself with a SMILE

Presenting your Poster

- Give your visitors a short **presentation/overview**
  - Your objectives
  - Your results
  - Handouts (optional)

- Don’t read your poster to your visitors

Presenting your Poster

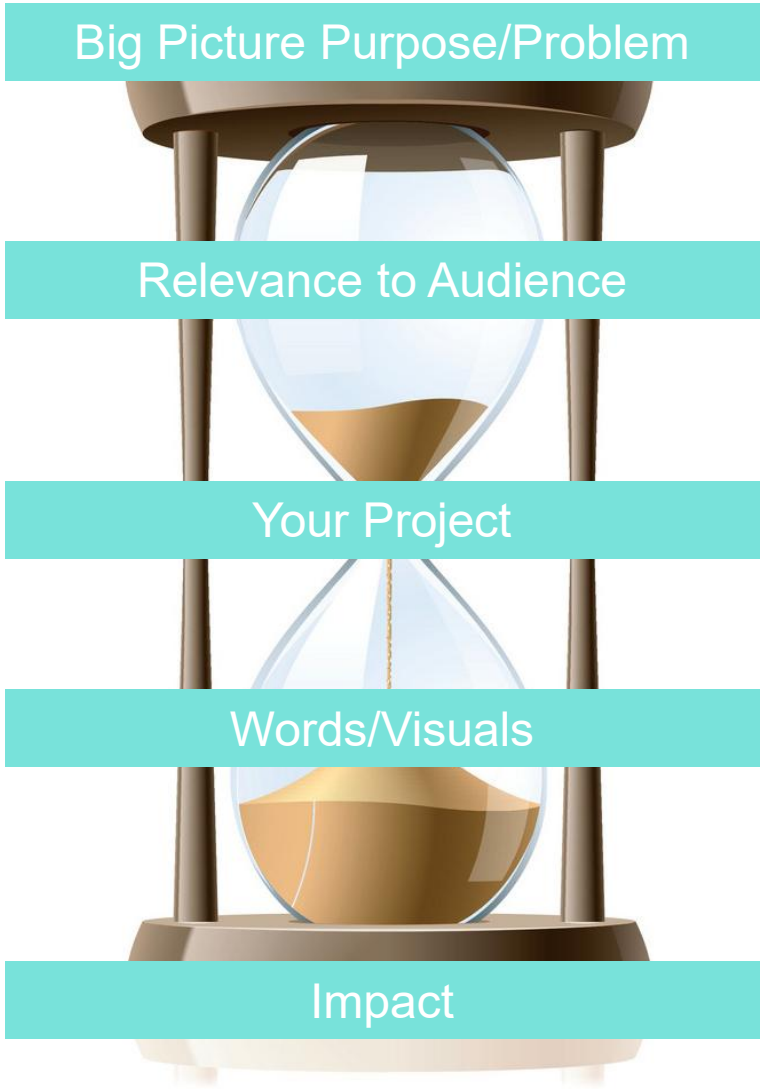

Carry your viewer along your research path while pointing out images and figures.

"The poster is not the centerpiece. Rather, it's the accessory to the story that comes out of the expert's mouth."

– Jordan Gaines, Neuroscientist